



EMPIR



The EMPIR initiative is co-funded by the European Union's Horizon 2020 research and innovation programme and the EMPIR Participating States

18SIP02 5GRFEX D1

Validation report on rigorous measurement capability for traceable RF-EMF measurement of massive MIMO systems for 5G base station applications based on RF-EMF measurement and data processing methods / protocols

Project Number: JRP 18SIP02

Project Title: Metrology for RF exposure from Massive MIMO 5G base station: Impact on 5G network deployment (5GRFEX)

Document Type: Deliverable Report

Authors: Tian Hong Loh, David Cheadle, Yunsong Gui, Fabien Heliot, and Michael Dieudonne

Lead Partner: NPL

Participating Partners: SURREY, Keysight DK

Due Date: September 2021

Submitted Date: December 2021

Table of Contents

| | | |
|-------|--|----|
| 1 | Scope of the document | 3 |
| 2 | Introduction | 3 |
| 2.1 | Background | 3 |
| 2.2 | Traceable measurement capability | 4 |
| 2.2.1 | mMIMO beamforming system | 5 |
| 2.2.2 | RF-EMF measurement systems..... | 6 |
| 2.3 | Measurands and factors considered..... | 7 |
| 2.4 | Measurement campaigns | 8 |
| 2.5 | Measurement methodologies | 8 |
| 3 | Indoor Measurement Campaign with mMIMO testbed | 11 |
| 3.1 | Indoor Measurement Campaign (1) | 11 |
| 3.1.1 | Measurement setup and test scenarios | 11 |
| 3.1.2 | Findings..... | 15 |
| 3.2 | Indoor Measurement Campaign (2) | 17 |
| 3.2.1 | Measurement setup and test scenarios | 17 |
| 3.2.2 | Findings..... | 19 |
| 3.3 | Indoor Measurement Campaign (3) | 23 |
| 3.3.1 | Measurement setup and test scenarios | 23 |
| 3.3.2 | Findings..... | 24 |
| 4 | Outdoor Measurement Campaign with mMIMO testbed | 25 |
| 4.1 | Outdoor Measurement Campaign (1) | 25 |
| 4.1.1 | Measurement setup and test scenario | 26 |
| 4.1.2 | Findings..... | 27 |
| 4.2 | Outdoor Measurement Campaign (2) | 32 |
| 4.2.1 | Measurement setup and test scenarios | 32 |
| 4.2.2 | Findings..... | 33 |
| 5 | Outdoor RF-EMF Measurement Campaign of 5G base station | 34 |
| 5.1 | Measurement setup and test scenarios | 34 |
| 5.2 | Findings | 43 |
| 6 | Conclusion | 46 |
| 7 | References..... | 47 |

List of Abbreviations

| | |
|---------|---|
| 3G | 3rd Generation Wireless Systems |
| 4G | 4th Generation Wireless Systems |
| 5G | 5th Generation Wireless Systems |
| CDF | Cumulative Distribution Function |
| CP-OFDM | Cyclic Prefix Orthogonal Frequency Division Multiplexing |
| CSI | Channel State Information |
| E-field | Electric field |
| EMF | Electromagnetic Field |
| ICNIRP | International Commission on Non-Ionizing Radiation Protection |
| IEEE | Institute of Electrical and Electronics Engineers |
| ITU | International Telecommunication Union |
| MIMO | Multiple-Input-Multiple-Output transmission |
| mMIMO | Massive Multiple-Input-Multiple-Output |
| MU-MIMO | Multi-user Multiple-Input-Multiple-Output transmission |
| NR | New Radio |
| PDF | Power Flux Density |
| QAM | Quadrature Amplitude Modulation |
| QPSK | Quadrature Phase-Shift Keying |
| RF | Radio Frequency |
| RF-EMF | Radio Frequency Electromagnetic Field |
| Rx | Receiving end |
| SSB | Synchronisation Signal Block |
| SSS | Secondary Synchronisation Signal |
| SU-MIMO | Single User Multiple-Input-Multiple-Output transmission |
| TDD | Time-Division Duplex |
| Tx | Transmitting end |
| UE | User Equipment |
| ZF | Zero forcing |

1 Scope of the document

This document, namely, Deliverable 1 (D1), serves as a validation report on work carried out under work package 1 (WP1) of the European Association of National Measurement Institutes (EURAMET) funded support for impact (SIP) project – 18SIP02, entitled “Metrology for RF exposure from Massive MIMO 5G base station: Impact on 5G network deployment (5GRFEX)”. This validation report presents the investigation of the impact on traceable radio frequency electromagnetic field (RF-EMF) measurements of massive multiple-input-multiple-output (mMIMO) systems for fifth generation (5G) base station (BS) applications. The rigorous measurement capability developed for traceable RF-EMF measurement of 5G new radio (NR) Massive MIMO base station systems based on RF-EMF measurement and data processing methods/protocols will be described. The main measurand considered is the RF-EMF whereby its link performance could be considered if the relevant information is available. The focus is given on establishing tracability and developing suitable RF-EMF measurement methods in the context of 5G mMIMO base stations serving two or more mobile users (i.e. multiple-user MIMO (MU-MIMO)) within realistic real-world environments and scenarios using the developed user-controllable mMIMO beamforming testbed and traceable RF-EMF measurement capability. Several RF-EMF measurement campaigns have been carried out (2 indoor and 2 outdoor) including the assessment of a 5G BS in an outdoor environment. During the measurement campaigns various varying factors such as number of users, position of users and data duty cycles are envisaged to be considered. Based on the experimental-based evidence on the stochastic nature of mMIMO, the measurement results are analysed statistically to enable the insight understanding, and the relevant conclusions are drawn regarding the proposed 5G measurement methodologies/protocols.

2 Introduction

2.1 Background

The 5G mobile networks, which promises high data rate, low latency and high reliability, is envisaged to be comprehensively rolled-out by 2020 [1]. The demand for high-speed communication for a range of diverse applications has driven strong global momentum in developing emerging 5G technologies to meet these needs. Current RF-EMF exposure limits have become a critical concern for 5G mobile network deployment across Europe. Regulation is not harmonized and in certain countries and regions goes beyond the guidelines set out by the International Commission on Non-Ionizing Radiation Protection (ICNIRP) [2].

The conventional measurements of RF-EMF exposure from third-generation (3G) and fourth-generation (4G) BSs at the exclusion zone (a compliance boundary around the BS with no access to general public), which are based on the assumption that the theoretical maximum power is transmitted in each possible direction for a defined timeperiod, are becoming obsolete [3]. This is due to the complex new technology employed at 5G base stations such as beamforming mMIMO, which allows energy to be focused with sharp high gain beams in the direction of a specific mobile user resulting in non-realistically large exclusion zone areas. This makes it problematic for operators to deploy 5G Massive MIMO BSs on sites with pre-existing 3G and 4G BSs.

Regulators, operators and 5G equipment suppliers all require reliable and agreed assessment of RF-EMF exposure levels to support consistent and effective 5G regulation and network design. Scientific arguments and effective RF-EMF measurements on a massive MIMO system will be needed to support this vision. It is envisaged that suitable statistical approaches should form the base of RF-EMF exposure assessment for 5G NR system employing mMIMO as beamforming in order to assure that high power user service beams are only transmitted on a need-to basis [3]–[5].

This project works towards producing guidance for RF-EMF exposure measurement of 5G mMIMO BSs. The objective is to obtain experimental-based evidence of stochastic nature of RF-EMF

exposure from these mMIMO system operating with downlink communications within a real-world environment and its quantification. It is important to note that the user-controllable mMIMO beamforming testbed is not a commercial base station and it enables user to have full control over its beamforming performance, which would definitely enable the project team to obtain a calibrated traceable RF-EMF measurement database to gain insight into the relevant statistics. Both indoor and outdoor environments would be considered whereby the focus is to provide insight into the statistical nature of RF-EMF exposure distribution, if feasible, over the whole area or some selected locations, and to assess into how their relevant changing exposure over time are affected by:

- the fluctuation of the environment,
- number and position of the different users,
- changes of data usage activities (i.e. data traffic pattern) of the active users.

Note that the user-controllable mMIMO beamforming testbed is envisaged to produce static beam(s) for different aforementioned factors whereas the live 5G BS system is envisaged to produce adaptive beam(s) without any specific knowledge on the beam patterns and its relationship with the aforementioned factors. The outcomes will be disseminated to technical, business and regulatory communities to support the development of effective regulation and enable 5G implementation that balances performance with public safety.

2.2 Traceable measurement capability

In this report, the following measurement capabilities, where applicable, incorporates the modified testbed capability developed in 14IND10 MET5G with Surrey's mMIMO systems have been employed:

- a user-controllable Surrey mMIMO beamforming system [6] with up to 128 channels transmit antenna array
- RF-EMF measurement systems:
 - up to 5 sets of Surrey 4-dipole-element receive antenna array each connect to a MegaBEE receiver
 - a handheld Keysight FieldFox N9917B portable spectrum analyser [7] and an AGOS SDIA-6000 triaxial isotropic field probe [8]

Figure 1 shows an illustrative setup photo of Surrey mMIMO Tx array with several RF-EMF MegaBEE receivers located on trolleys operating with multiple dipole antenna elements.

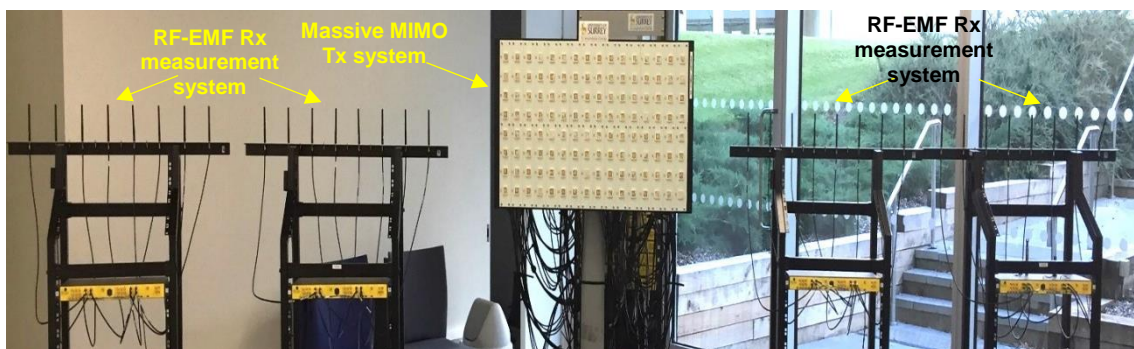


Figure 1 *Surrey transmit array (centre) with several RF-EMF MegaBEE receivers located on trolleys operating with multiple dipole elements.*

To achieve tracability, all these antenna and systems have been calibrated. The Keysight RF-EMF measurement system was calibrated at the UK National Physical Laboratory (NPL) in its Power Flux Density (PDF) laboratory against known generated Electric field (E-field) [9] whereas the Surrey RF-EMF measurement systems were calibrated component-wise with separate measurements made on

the cables, MegaBEE receivers and antennas. The 4-dipole-element receiver antenna arrays were calibrated by using the three antenna method. The MegaBEE receivers were calibrated for sensitivity to RF power received using power sensor. See the Deliverable report D2 for details of the relevant calibration methods and setup.

2.2.1 mMIMO beamforming system

The mMIMO beamforming system consists of: 1) A BEE7 synchronization and trigger generator; 2) A MegaBEE transceiver module (each module contains four input/output RF ports and could support up to 4 channels of IQ); 3) A White Rabbit time distribution system; 4) A transmit antenna array with 128 (16×8) patch antenna elements.

The mMIMO testbed can perform phase-coherent (after the OTA mMIMO phase coherency calibration) and time synchronized MIMO baseband processing with user-programmable, reconfigurable and real-time signal processing field-programmable gate arrays (FPGAs)-based software defined radio (SDR) capabilities.

For downlink communications, up to 128 channels could be used simultaneously at the transmitting end by using all the 32 transceiver modules whereas, at the receiving end, up to 32 channels can be used.

The synchronization of the mMIMO testbed is controlled by the BEE7 synchronization and a trigger generator. The signal generation and analysis are all implemented using the MegaBEE transceivers. The clocking network that achieves sub-nano second time synchronization between channels is derived from the White Rabbit time distribution system, which synchronizes a reference clock to each of the MegaBEE transceiver modules over an optical fibre link using SFP+ (Small Form-factor Pluggable Plus) network adaptors. Note that optical fibers are employed for both data transport and the clocking network. Figure 2 shows a photo of the Surrey mMIMO beamforming system. The following shows some current key system features for MIMO downlink configuration:

- RF operating frequency centric at 2.63 GHz
- CP-OFDM (Cyclic Prefix Orthogonal Frequency Division Multiplexing) waveform matching a 5G NR configuration
- Data frame generation with pilot signals
- 40 MHz instantaneous data bandwidth per channel
- Subcarrier spacing of 15 kHz in time division duplex (TDD) mode
- Symbol modulation formats: QPSK, 16-QAM, 64-QAM
- Flexible Massive MIMO as Tx (transmitting end) configuration for 16 up to 96 Antennas
- Flexible Receiver system as Rx (receiving end) configuration for up to 20 Antennas
- MATLAB baseband processing, algorithmic evaluation and zero-forcing beamforming
- Receive antennas separated by several wavelength distance
- Capable of MIMO precoding at Tx and channel estimation with receive pilots at Rx
- Transmission rate at 61.44 MSps for a fixed length of 65536 samples (i.e. 2^{16})

This testbed is capable of mimicking the performance of a realistic 5G BS. The testbed provides flexible evaluation of various modulation schemes, new communication algorithms and protocols as well as enabling evaluation of the relevant OTA link performance.

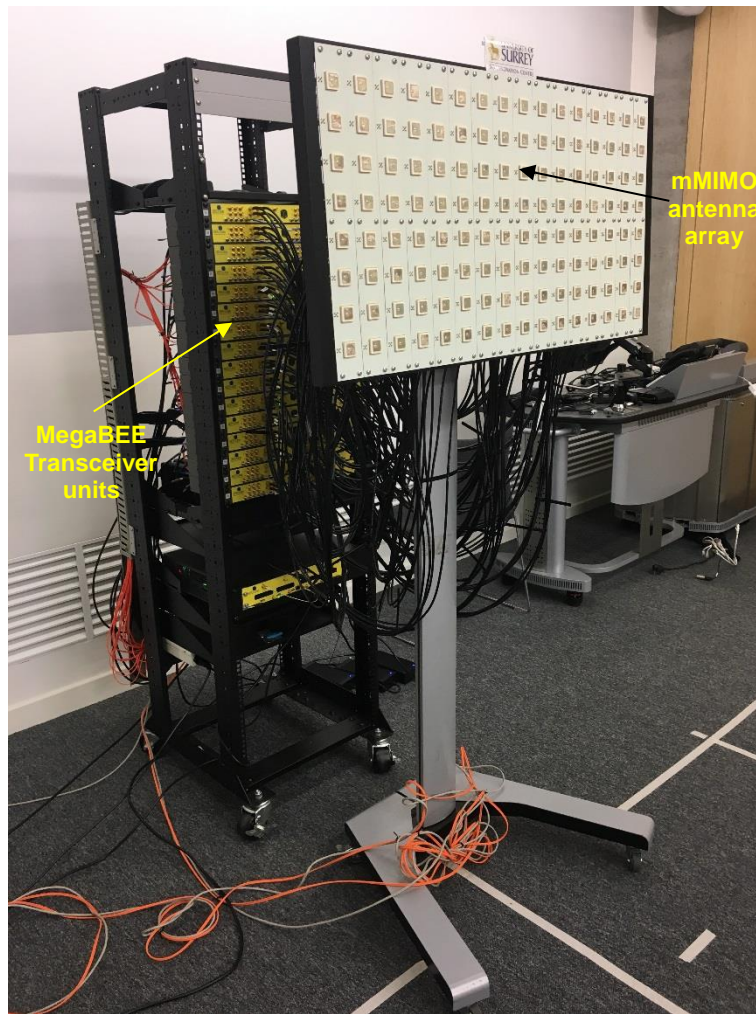


Figure 2 *Surrey mMIMO beamforming system.*

2.2.2 RF-EMF measurement systems

The Surrey RF-EMF measurement system consists of up to five sets of 4-dipole-element receive antenna array. Figure 3 shows a photo of the Keysight RF-EMF measurement system, in which the channel power could be acquired, consists of a handheld Keysight FieldFox N9917B portable spectrum analyser [7], and an AGOS SDIA-6000 triaxial isotropic field probe [8] (allocated on a tripod as depicted in Figure 3(b)). Note that the power measurement acquired by the Keysight RF-EMF measurement system will be used as a calibrated reference for the measurement campaigns.

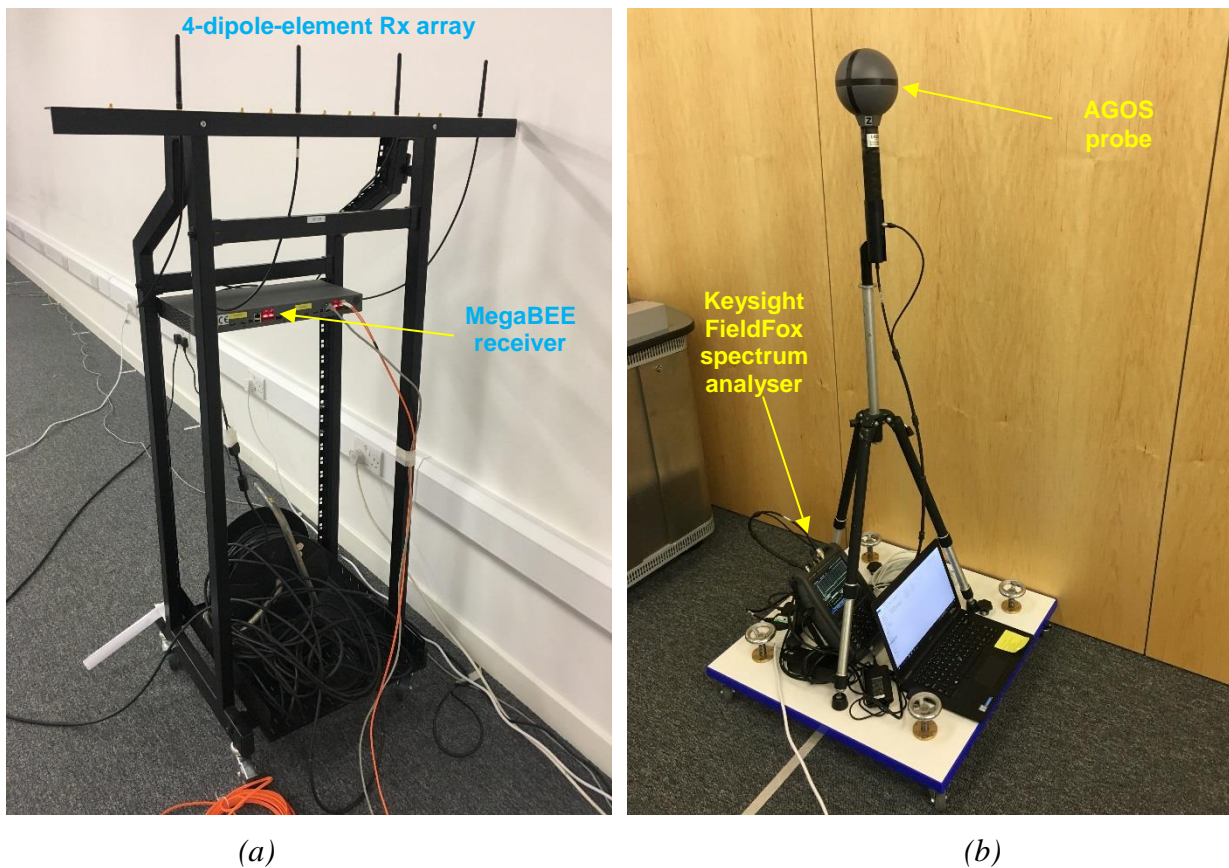


Figure 3 Photos of the: (a) Surrey RF-EMF measurement system; (b) Keysight RF-EMF measurement system.

2.3 Measurands and factors considered

The following are the envisaged measurands:

1. RF-EMF (could be calculated by acquiring the received channel power and then converting it into power density for obtaining of RF-EMF)
2. Link performance (e.g. BER, EVM, etc.)¹

The following are the factors to be considered:

1. Spatial RF-EMF variation at different locations (with receiver located at grid location this takes the fluctuation of the environments into account)
2. Temporal RF-EMF variation at a fixed location
3. Different sized mMIMO system operation (e.g. 16x16, 32x32, etc. Only with Surrey's mMIMO)
4. Number and position of active users
5. Data usage activities (i.e. data traffic pattern) of the active users
6. Different scenarios: line-of-sight (LOS), non-line-of-sight (NLOS), etc.

¹ Note that, in this project, this parameter is optional and only could be acquired with Surrey's receiver systems.

(1) Indoor:

- (i) Fixed position of Surrey RF-EMF receivers distributed in the field of interest (see example layout in Figure 4)
 - With both Keysight's and Surrey's RF-EMF systems as calibrated & traceable RF-EMF tool, perform all RF-EMF measurement using these systems and validate the measurement results against each other.
 - Transmit a beam with different combination of the following parameters:
 - User number, e.g. 1, 2, 3, 4, 5
 - User position, e.g. beam pointing at -45° , 0° , 45°
 - Traffic profile, e.g. 20%, 40%, 60%, 80%, 100% resource block allocation per user
- (ii) Change the physical position of the Surrey RF-EMF Rx system and/or the Keysight Rx system, re-run step (i), i.e. the RF-EMF measurements with same variations.

(2) Outdoor:

- (i) Same as (1) but outside the building without blocking objects (i.e. LOS scenarios)
- (ii) Same as (1) but outside the building with blocking objects (i.e. NLOS scenarios)

Note that for the outdoor measurement campaign, the maximum test area is restricted by the length of the synchronisation cables. Where possible, an investigation will also be performed by repeating a sub-set of the outdoor measurement campaign with mMIMO system moves to different location so to assess the effects on RF-EMF due to the change of beamforming conditions. Depending on the time available and feasibility for carry out the measurement campaign, the project teams would envisage to operate the Surrey's mMIMO Tx system to produce static beam for acquiring the associated RF-EMF considering the combination of the following varying factors for statistical study of experimental-based evidence of stochastic nature of mMIMO and its quantification:

- Number of virtual active users: Up to 5 (i.e. generate up to 5 beams)
- Position of virtual active users: Up to 5 (i.e. 5 positions)
- Data Traffic Pattern of frame: Up to 5 different data rate each user (e.g. 20%, 40%, 60%, 80%, 100%)

Figure 5 shows some illustrative diagrams on how virtual beamforming are formed considering the aforementioned varying factors. Note that both the Keysight and Surrey RF-EMF systems have been calibrated whereby it is envisaged that the measured results could be used for cross validation. Virtual users (red dot) are not having a real receiver on that point, the beams are pre-computed and loaded/transmitted in a static way to the field of interest for the duration of the measurement. Also, the static beams are computed taking with different traffic profiles and quantity of virtual users. Table 1 below shows the envisaged example configurations of the data traffic profile (in unit of %) for each user for scenario shown in Figure 5 (e).

Table 1 Example configurations of the data traffic profile.

| Measurement No | 1 | 2 | 3 | 4 | 5 | 6 | 7 | 8 | 9 | 10 | ... | 21 | 22 | 23 | 24 | 25 | 26 | 27 | 28 | 29 | 30 | ... | 625 |
|----------------|----|----|----|----|-----|----|----|----|----|-----|-----|-----|-----|-----|-----|-----|----|----|----|----|-----|-----|-----|
| User 1 | 20 | 40 | 60 | 80 | 100 | 20 | 40 | 60 | 80 | 100 | ... | 20 | 40 | 60 | 80 | 100 | 20 | 40 | 60 | 80 | 100 | ... | 100 |
| User 2 | 20 | 20 | 20 | 20 | 20 | 40 | 40 | 40 | 40 | 40 | ... | 100 | 100 | 100 | 100 | 100 | 20 | 20 | 20 | 20 | 20 | ... | 100 |
| User 3 | 20 | 20 | 20 | 20 | 20 | 20 | 20 | 20 | 20 | 20 | ... | 20 | 20 | 20 | 20 | 20 | 40 | 40 | 40 | 40 | 40 | ... | 100 |
| User 4 | 20 | 20 | 20 | 20 | 20 | 20 | 20 | 20 | 20 | 20 | ... | 20 | 20 | 20 | 20 | 20 | 20 | 20 | 20 | 20 | 20 | ... | 100 |

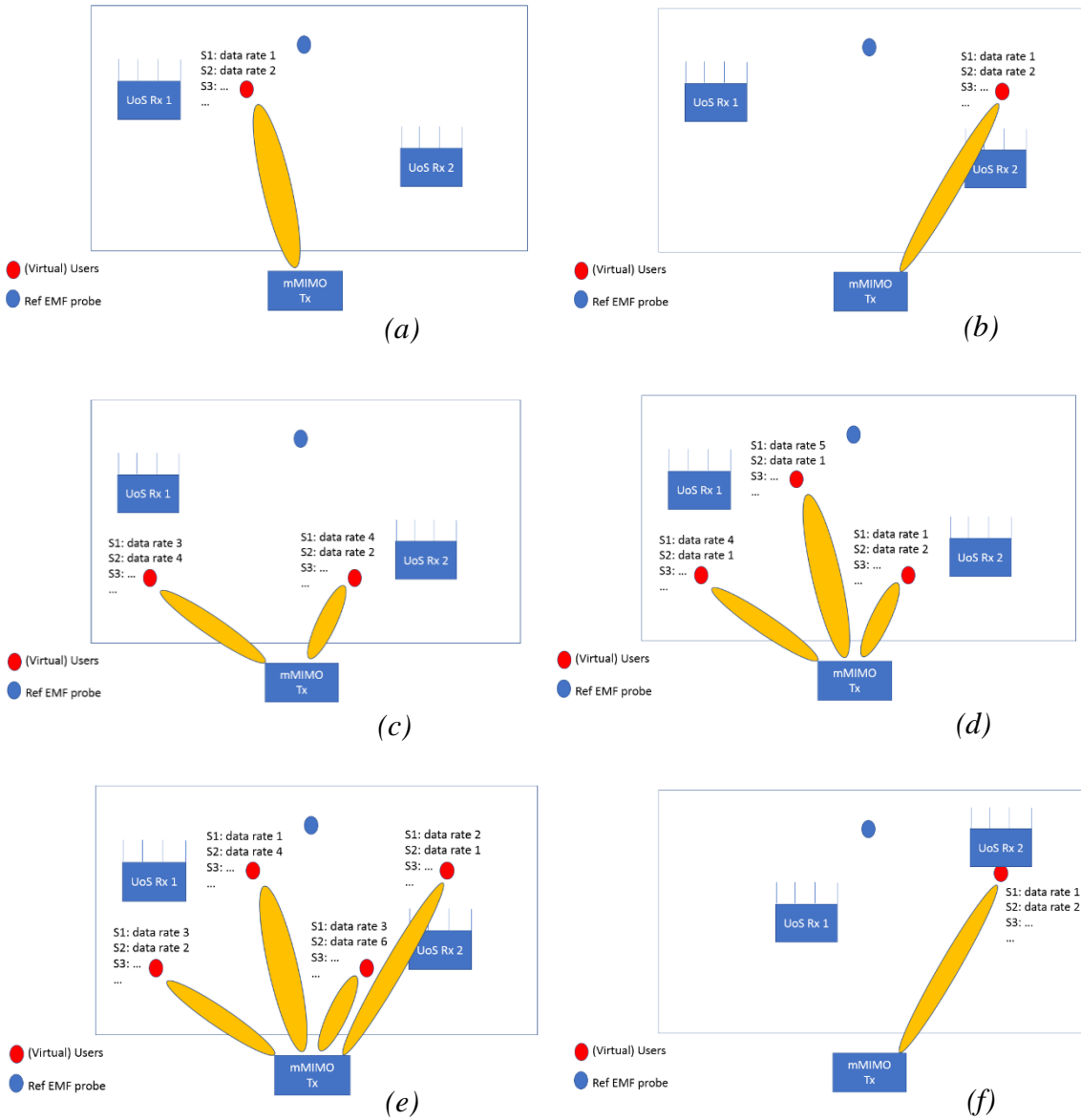


Figure 5 Illustrative diagrams showing virtual beamforming scenarios for different number of users, user data rate, and user location. See Figure 1 for the considered measurement grid topology.

A suitable statistical approach over data processing would be carried out following the measurement campaigns to try to make sensible conclusions based on observations found from the measured results obtained.

3 Indoor Measurement Campaign with mMIMO testbed

3.1 Indoor Measurement Campaign (1)

For this first indoor measurement campaign [10], all the measurements were performed inside an indoor environment within a large meeting room, located at the basement of the 5G Innovation Centre (5GIC) at the University of Surrey. The room is 15 m long, 7.5 m wide, and 3 m high. The typical furniture, such as chairs, and desk within the room were placed aside during the measurements. The room is surrounded by glass, brick and plasterboard walls.

3.1.1 Measurement setup and test scenarios

Figure 6 shows the relevant indoor environment and measurement grid. The floor is made of concrete and carpeted. The concrete suspended ceiling was equipped with some hanging lighting and projector equipment. During the measurement, all the measurement instruments were located inside the room. The measurements are performed within an $8\text{ m} \times 6\text{ m}$ area, which is divided into a grid of 48 square of 1 m for the ease of measurement, as is depicted in Figure 6.

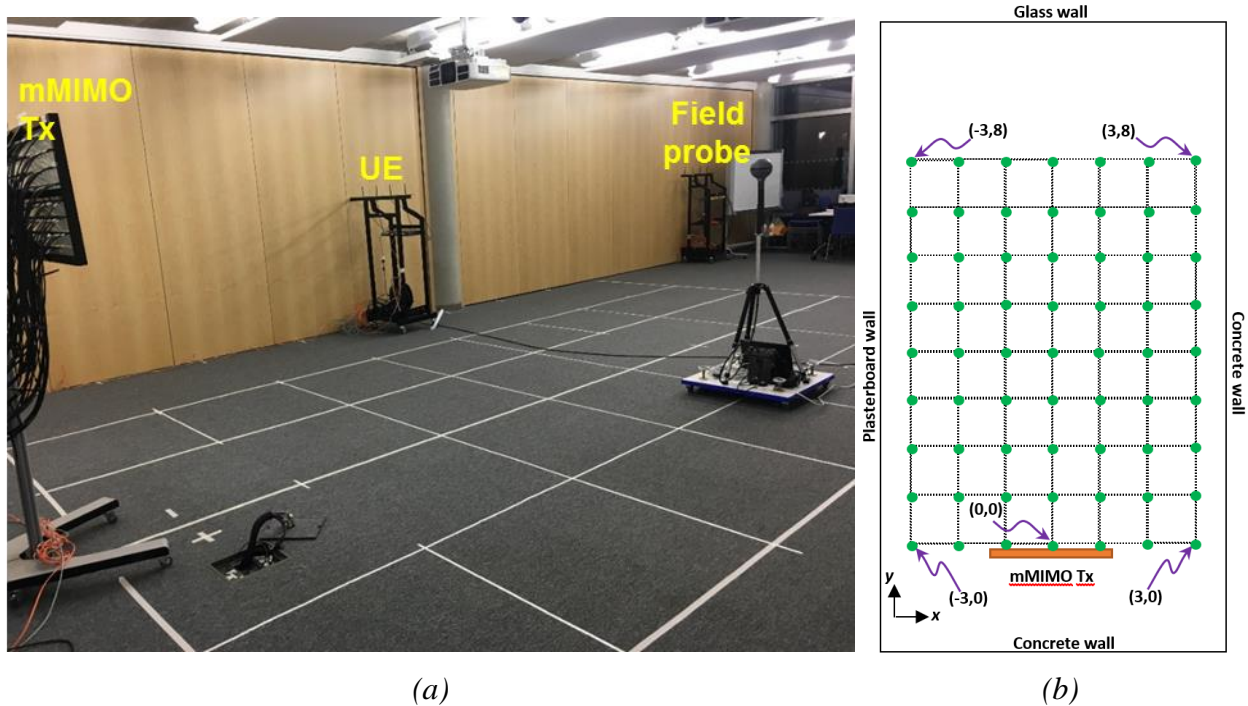


Figure 6 *The relevant indoor environment and the measurement grid.*

The mMIMO Tx system was configured to operate with 64 active transmitting antennas. The RF-EMF measurement system was located on a trolley during the measurement (see Figure 6(a)). The mMIMO Tx system was programmed to perform downlink zero forcing (ZF) precoding after channel state information (CSI) acquisition for different beamforming scenarios with respect to the associated user terminal antenna setups and positions. Using a calibrated triaxial isotropic field-probe as part of the Keysight RF-EMF measurement system, the received channel power heat map for each beamforming scenario was acquired and then converted into an RF-EMF heat map. The following shows the relevant MIMO downlink configuration setting employed in this measurement campaign:

- 64 active mMIMO Tx with real-time transmission
- 4-dipole-element Rx antenna array each with a MegaBEE receiver (which act as ‘user equipment (UE)’ for stimulating beam pointing direction/location)
- RF operating frequency centric at 2.63 GHz
- 40 MHz instantaneous data bandwidth per channel
- OFDM frames with subcarrier spacing of 15 kHz in TDD mode
- Transmission rate at 61.44 MSps for a fixed length of 65536 samples (i.e. 2^{16})
- Symbol modulation formats: QPSK, 16-QAM and 64-QAM
- Keysight RF-EMF measurement system (Spectrum analyser and triaxial isotropic field-probe)
- MATLAB baseband processing and zero-forcing beamforming

The following beamforming scenarios for single-user (SU) and multi-user (MU) downlink communications at different locations have been considered: 1) SU at (0 m, 8 m); 2) SU at (-3 m, 4 m); 3) SU at (3 m, 2 m); 4) MU at (-3 m, 4 m) and (3 m, 2 m); 5) MU at (0 m, 8 m) and (0 m, 4 m); 6) MU at (0 m, 8 m) and (-3 m, 4 m); 7) MU at (0 m, 8 m) and (3 m, 2 m); 8) MU at (0 m, 8 m), (-3 m, 4 m) and (3 m, 2 m). Figure 7 illustrates the two MU setup examples (i.e. Scenarios 5 and 8), where the received channel power heat map was acquired by ensuring a consistent Keysight RF-EMF probe orientation throughout all the measured grid points (shown as green dots in the Figure 6 and Figure 7).

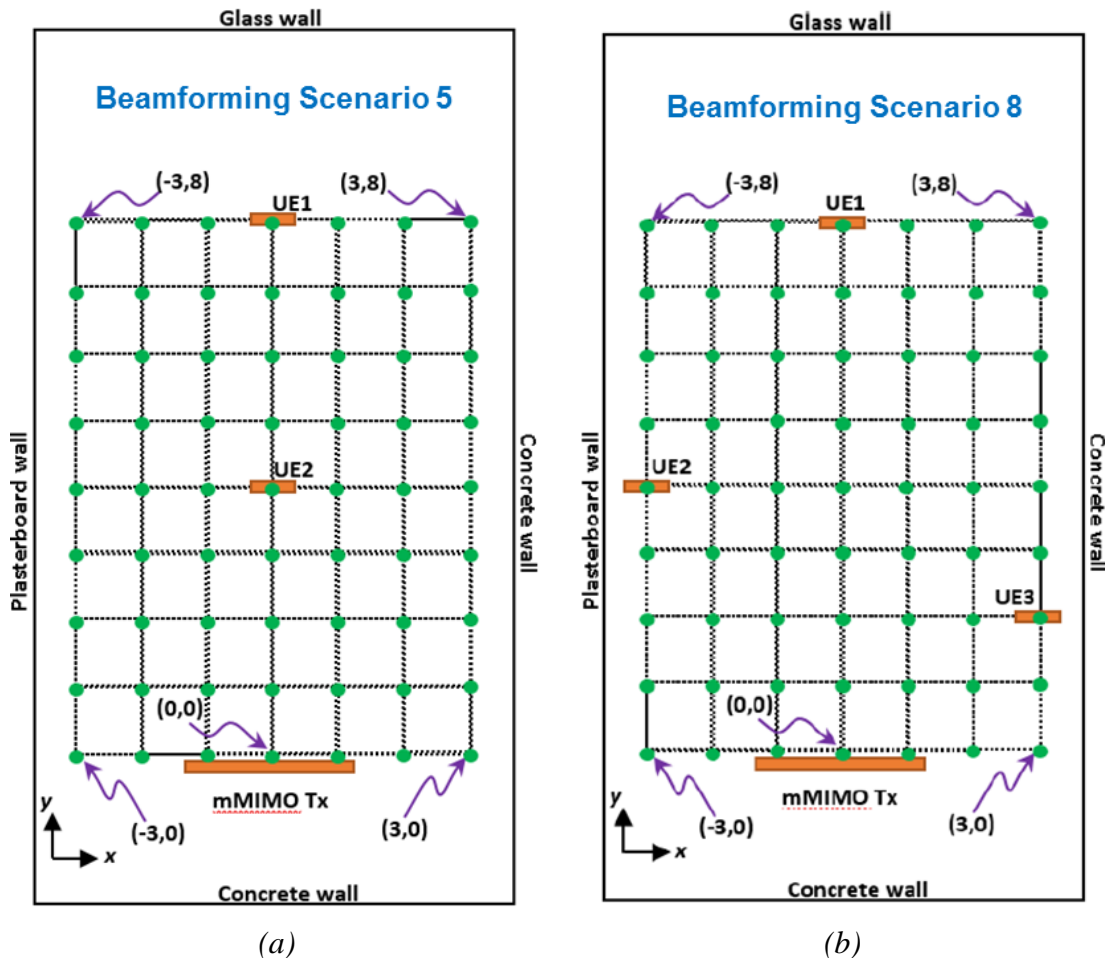


Figure 7 Test scenarios for 64 active mMIMO Tx at $(0\text{ m}, 0\text{ m})$: (a) 2 active beams at $(0\text{ m}, 8\text{ m})$ and $(0\text{ m}, 4\text{ m})$; (b) 3 active beams at $(0\text{ m}, 8\text{ m})$, $(-3\text{ m}, 4\text{ m})$ and $(3\text{ m}, 2\text{ m})$.

Figure 8 illustrates the relevant eight static beam scenarios that vary number of active users and their position (i.e. beam profile). Figure 9 shows photos of some relevant setups. The acquired channel power results for each beamforming scenario have then been converted into a corresponding RF-EMF heat map. For each beamforming scenario considered, the same measurement procedure was followed:

- (1) first a pilot frame is sent from the mMIMO Tx system to each receiving location, which acquires and feedback its CSI via the SFP+ cable;
- (2) the mMIMO Tx system then estimates the CSI and uses it to generate ZF precoded data frame;
- (3) finally the mMIMO Tx system transmits these ZF precoded data frames in a continuous manner while the probe is moved to the 56 different grid positions of Figure 6 to measure the RF-EMF.

In order to ensure that the ZF precoding reasonably well, the uncoded bit-errorrate (BER) when using a 64-QAM is calculated at each UE based on the first received data frame. Note that the power level of the mMIMO Tx system is normalized for all the above measurements.

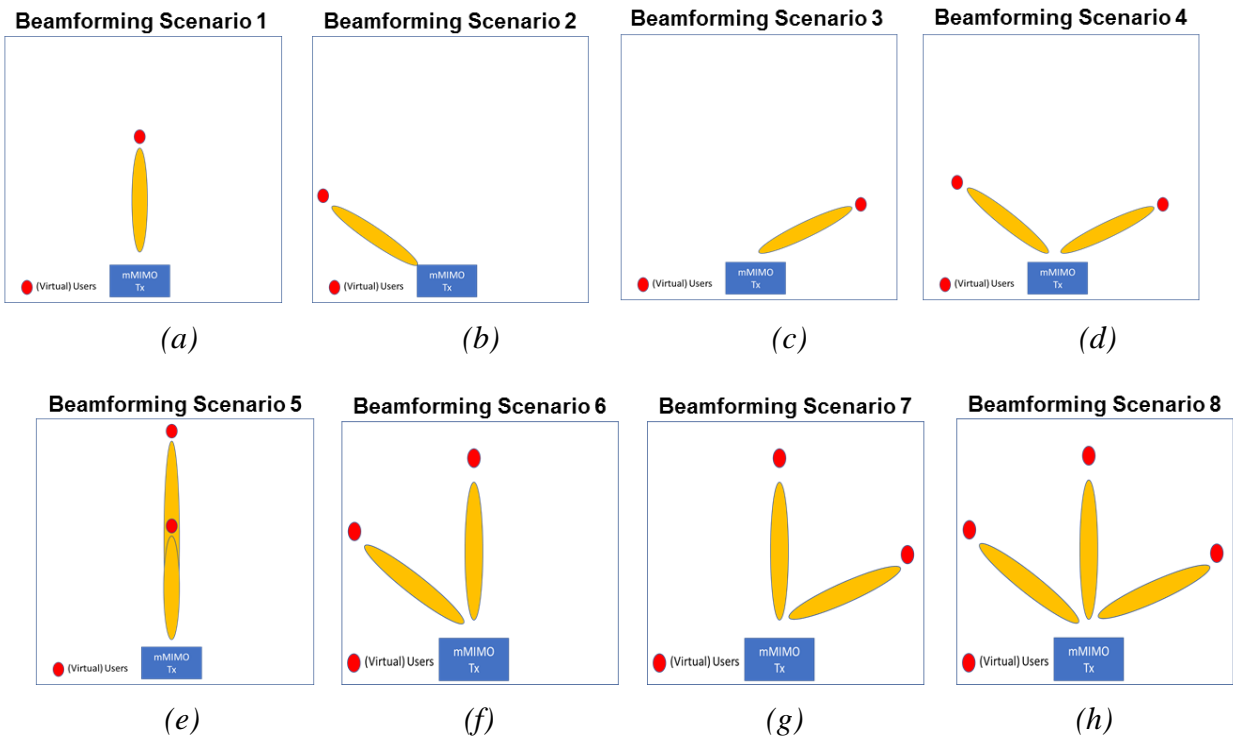
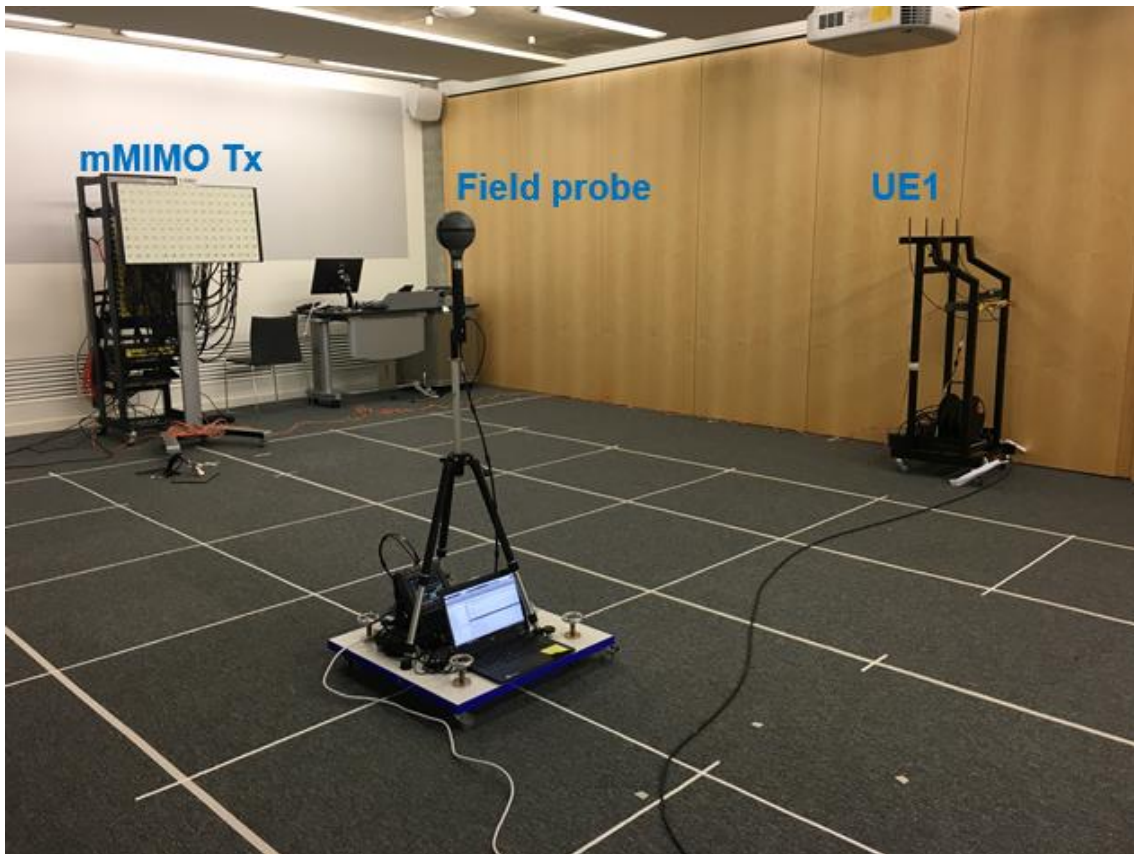


Figure 8 All the test scenarios for 64 active mMIMO Tx at $(0\text{ m}, 0\text{ m})$: (a) 1 active beam at $(0\text{ m}, 8\text{ m})$; (b) 1 active beam at $(-3\text{ m}, 4\text{ m})$; (c) 1 active beam at $(3\text{ m}, 2\text{ m})$; (d) 2 active beams at $(-3\text{ m}, 4\text{ m})$ and $(3\text{ m}, 2\text{ m})$; (e) 2 active beams at $(0\text{ m}, 8\text{ m})$ and $(0\text{ m}, 4\text{ m})$; (f) 2 active beams at $(0\text{ m}, 8\text{ m})$ and $(-3\text{ m}, 4\text{ m})$; (g) 2 active beams at $(0\text{ m}, 8\text{ m})$ and $(3\text{ m}, 2\text{ m})$; (h) 3 active beams at $(0\text{ m}, 8\text{ m})$, $(-3\text{ m}, 4\text{ m})$ and $(3\text{ m}, 2\text{ m})$.



(a)



(b)

Figure 9 Photos of the experimental setup for: (a) 1 active UE at $(-3 \text{ m}, 4 \text{ m})$; (b) 3 active UEs at $(0 \text{ m}, 8 \text{ m})$, $(-3 \text{ m}, 4 \text{ m})$ and $(3 \text{ m}, 2 \text{ m})$.

3.1.2 Findings

Table 2 presents the bit error rate (BER) values at each UE for each beamforming scenario; the results show that when using ZF precoding, the more the users, the lower the quality of the beamforming. But still in any case uncoded BER of around 10^{-3} can be achieved, which tend to confirm that the BS beamforms in the expected direction.

Table 2 BER of each UR for each beamforming test scenario listed in Section 3.1.

| Scenario | UE1 | UE2 | UE3 |
|----------|-----------------------|-----------------------|-----------------------|
| (1) | 1.35×10^{-6} | N/A | N/A |
| (2) | 4.61×10^{-6} | N/A | N/A |
| (3) | 5.12×10^{-6} | N/A | N/A |
| (4) | 2.35×10^{-6} | 4.82×10^{-5} | N/A |
| (5) | 8.38×10^{-5} | 9.22×10^{-5} | N/A |
| (6) | 3.68×10^{-5} | 4.31×10^{-5} | N/A |
| (7) | 4.37×10^{-5} | 3.99×10^{-5} | N/A |
| (8) | 8.04×10^{-4} | 2.68×10^{-3} | 5.11×10^{-4} |

Figure 10 depicts the received constellation in scenario (1) for Quadrature Phase-Shift Keying (QPSK), 16 Quadrature Amplitude Modulation (16-QAM) and 64-QAM, which confirm the high link quality. The calibrated RF-exposure results for the eight beamforming scenarios as well as their average, based on the field probe measurements of the received channel power at each grid point, are presented in Figure 11 by means of a heat map. The intensity of the RF-exposure is expressed in V/m and is colour-coded to illustrate its variation at different points of the room. In each subplot, the circle(s) represent the position of the active beam(s).

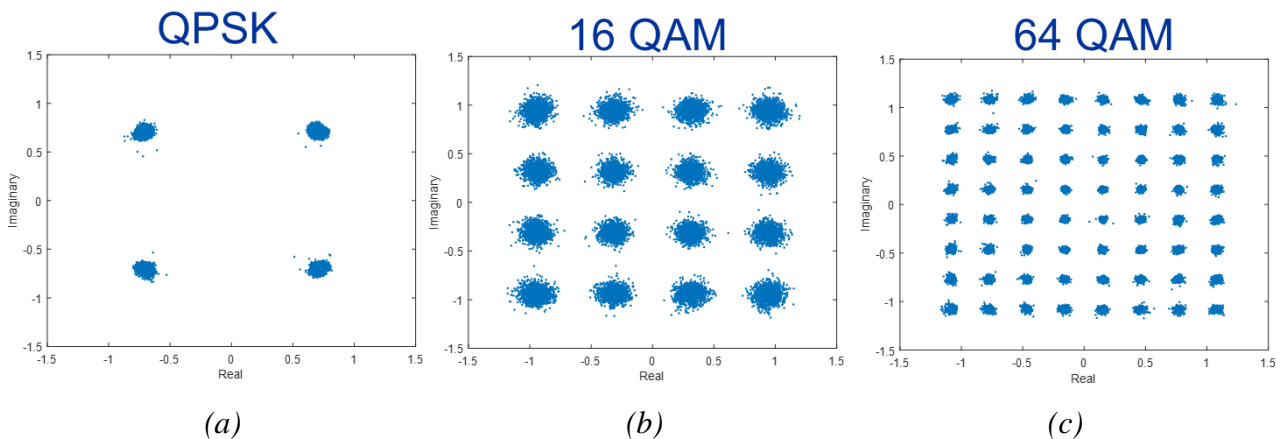


Figure 10 Received constellation in Scenario (1): (a) QPSK; (b) 16-QAM; (c) 64-QAM.

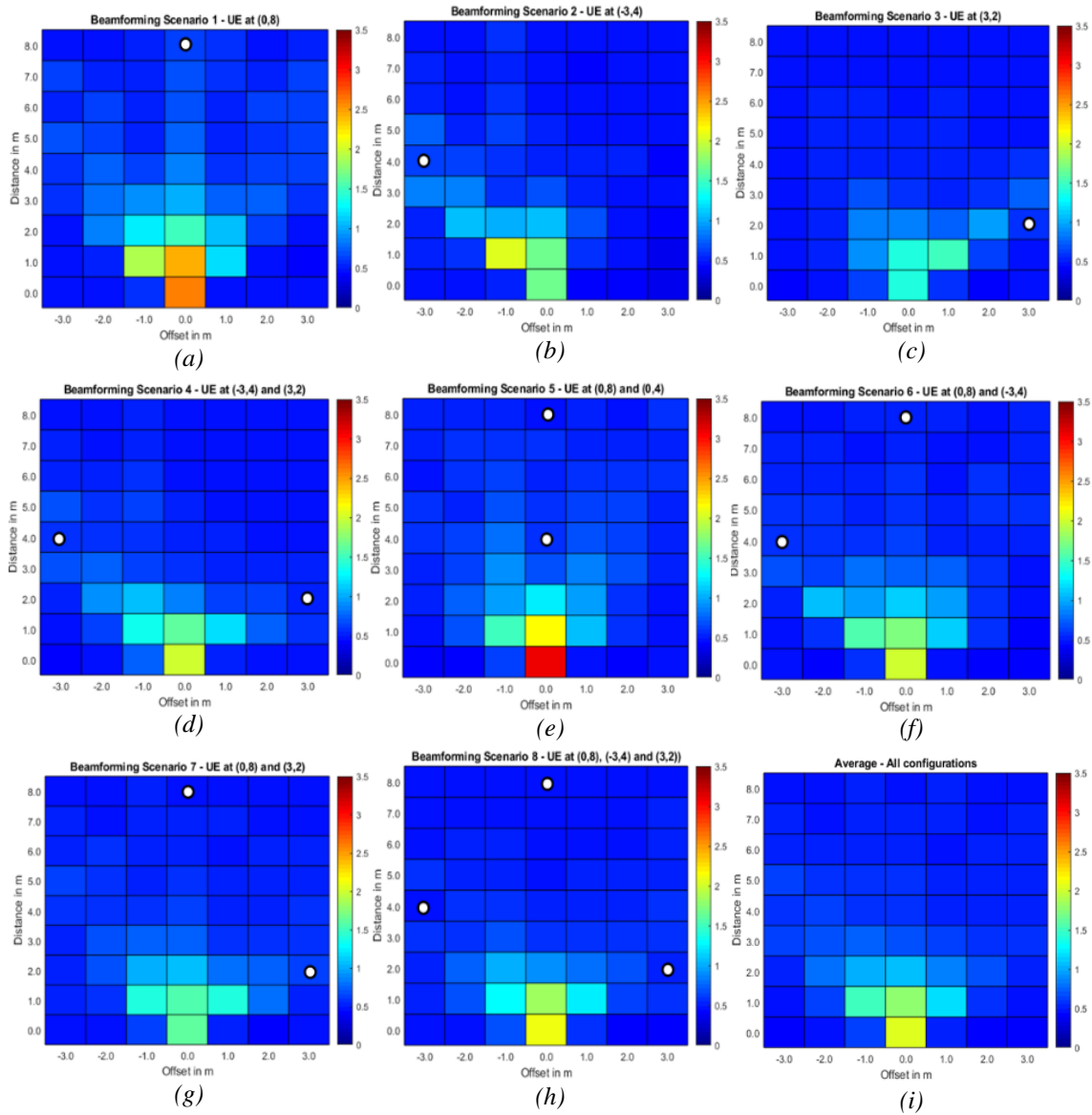


Figure 11 Calibrated RF-EMF heat map [colour map value shown in V/m] for (a)-(h) the 8 beamforming scenarios mentioned in Section 3.1; (i) their average value. Note that the white circle shown in the plots depicts the beam pointing directions.

The results show that an mMIMO BS does not generate a uniform RF-exposure as a traditional BS will do, but the exposure pattern follows more or less the envisaged ‘beam profile’. However, as for a traditional BS, the higher exposure levels are concentrated in the vicinity of the BS, i.e. the highest level of RF-exposure generated by the 64-Tx mMIMO BS is localised at (0 m, 0 m) in most cases, where the mMIMO BS is located. In order to get some statistical insights from the RF-exposure results, the results for an offset 0 m and a distance varying from 0 to 8 m, i.e. along the red arrow of Figure 11(i), are plotted for all the scenarios and average in Figure 12.

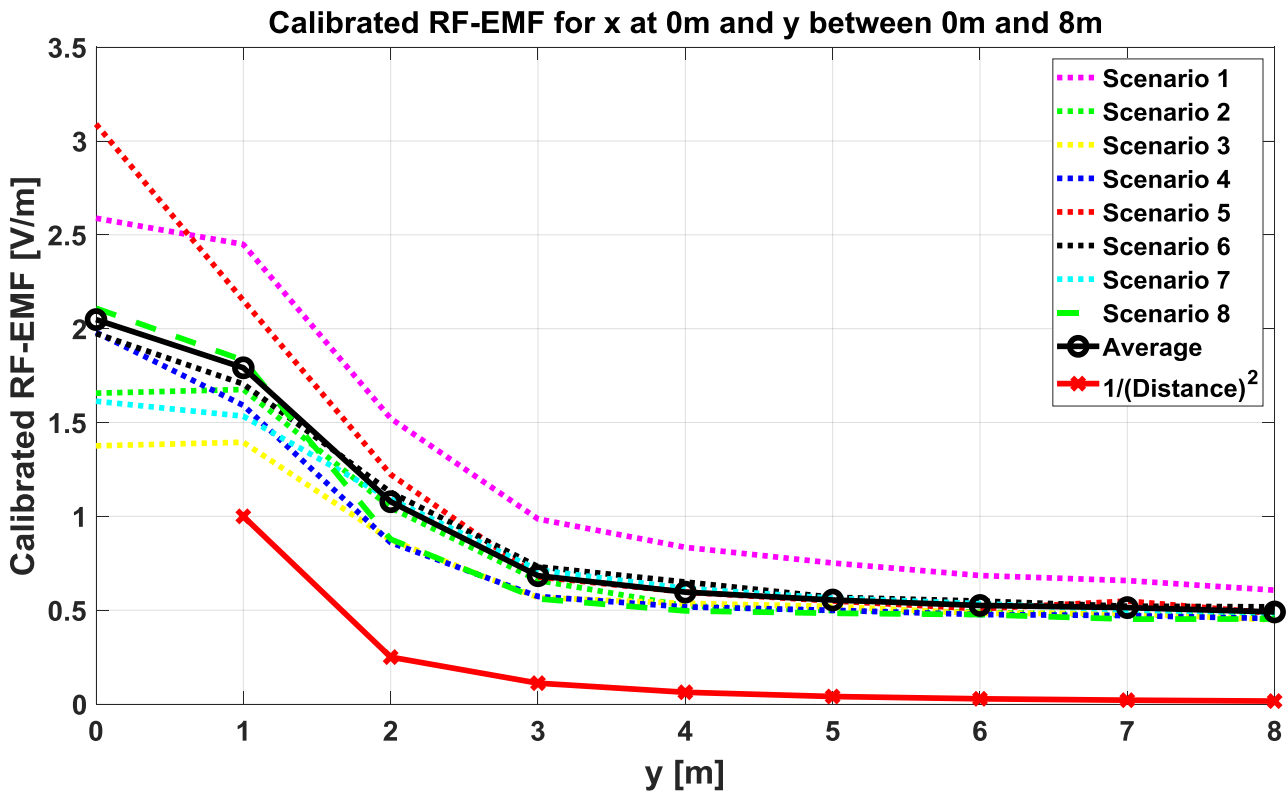


Figure 12 Calibrated RF-exposure of all scenarios for an offset of 0 m and a distance varying from 0 to 8 m.

The general trend, in all cases, is that the RF-exposure is inversely proportional to the square of the transmission distance, even when there is no main beam pointing directly into this direction, i.e. scenario (4). It is also interesting to note that the scenario generating the most RF-exposure among all the scenarios is scenario (1), where the BS transmits only to one beam in the main direction studied in Figure 12. On the other hand, in Scenario (5) with two beams in the main direction or scenarios (6), (7) and (8) with at least one active beam in the main direction, the mMIMO BS generates less RF-exposure than scenario (1). This tends to imply that the more active beams are served, the more the RF-exposure could be spread and hence be less intense. It can also be noted that the exposure varies between 1.37 and 3.09 V/m in these indoor scenarios.

3.2 Indoor Measurement Campaign (2)

Contrary to the first experiment, the second experiment is more comprehensive and study, for instance, the impact of the number of beams or the user traffic load with non-ideal mMIMO beamforming operation on the RF-exposure based on a very large amount of acquired data [11]. The other differences are fully detailed in the following.

3.2.1 Measurement setup and test scenarios

In the second experiment, the mMIMO BS operates with 96 active transmitting antennas, while each receiver operates with four dipole receiving antennas. Contrary to first experiment where the receivers were considered to be UEs, i.e. receiving pilot signals and feed backing the CSI to the BS such that it can steer beams towards them, the receivers are here used as extra probes to measure the RFexposure at the location they are placed whilst the mMIMO BS is not necessarily transmitting/steering a beam towards them; this allows to acquire more measurements and get a better statistical view of the RF-exposure. During the measurement campaign, various SU and MU MIMO

downlink communication beamforming scenarios were considered, with different combinations of active beams and data traffic loading to mimic the performance of a realistic 5G BS. The RF-exposure was measured by using five receivers and the probe placed at different locations within the grid, as it is depicted in Figure 13. In Figure 13, Rx # indicates the receiver number with its corresponding IP address, while P1 represents the probe.

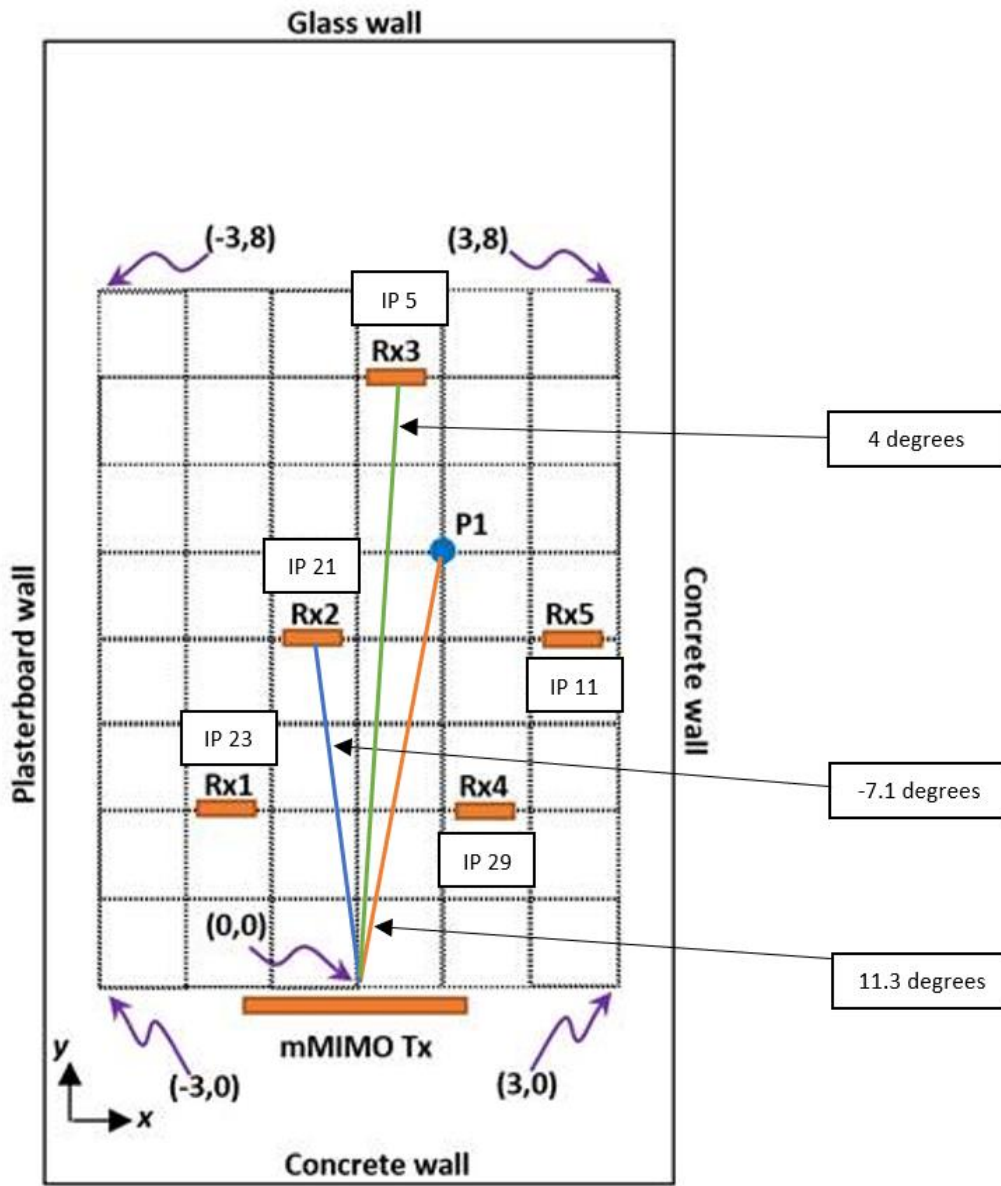


Figure 13 Measurement setup for 96 active mMIMO Tx at (0 m, 0 m), the five receivers and the probe.

In this measurement campaign, fully compliant 5G NR waveforms are used to transmit data. The 5G NR beamforming baseband signals are generated by using Keysight PathWave System Design platform (also known as SystemVue) [12]. This software can be used to generate up to 19 potential beam directions equally spaced every 5° between ±45° in azimuth and elevation=0°. Each generated beam contains a physical downlink shared channel with a configurable data payload that is transmitted within a 1-ms period. The data rate of each beam payload can be controlled by adjusting the modulation coding scheme, i.e. QPSK, 16-QAM, 64-QAM, as well as the number of allocated resource blocks (NRBs) used in the transmission. In the experiment, up to 216 NRBs are used per beams and up to 4 out of the 19 beams are active simultaneously to mimic an mMIMO BS beamforming data transmission towards up to 4 active users at the same time. Note that up to 864

total NRBS are used for 4 simultaneously active beams and the power level of the mMIMO Tx system is not normalized. As in the first experiment, the carrier frequency of the downlink transmission is 2.63 GHz with a bandwidth of 38.88 MHz, and a subcarrier spacing of 15 kHz.

One envisages that the variations of the beam profiles and data rates are useful for assessing the spatial variation of RF-exposure surrounding the mMIMO testbed. In order to get insights into the effect on the stochastic nature of RF-exposure generated by the non-ideal mMIMO beamforming operation due to potential hardware impairments and/or other factors (i.e. the beams may not be well defined and may not steer in the expected direction) in the studied environment, tens of thousands of E-field measurements were acquired, after the multi-channel OTA calibration had been performed, with random active beams and payload data rate.

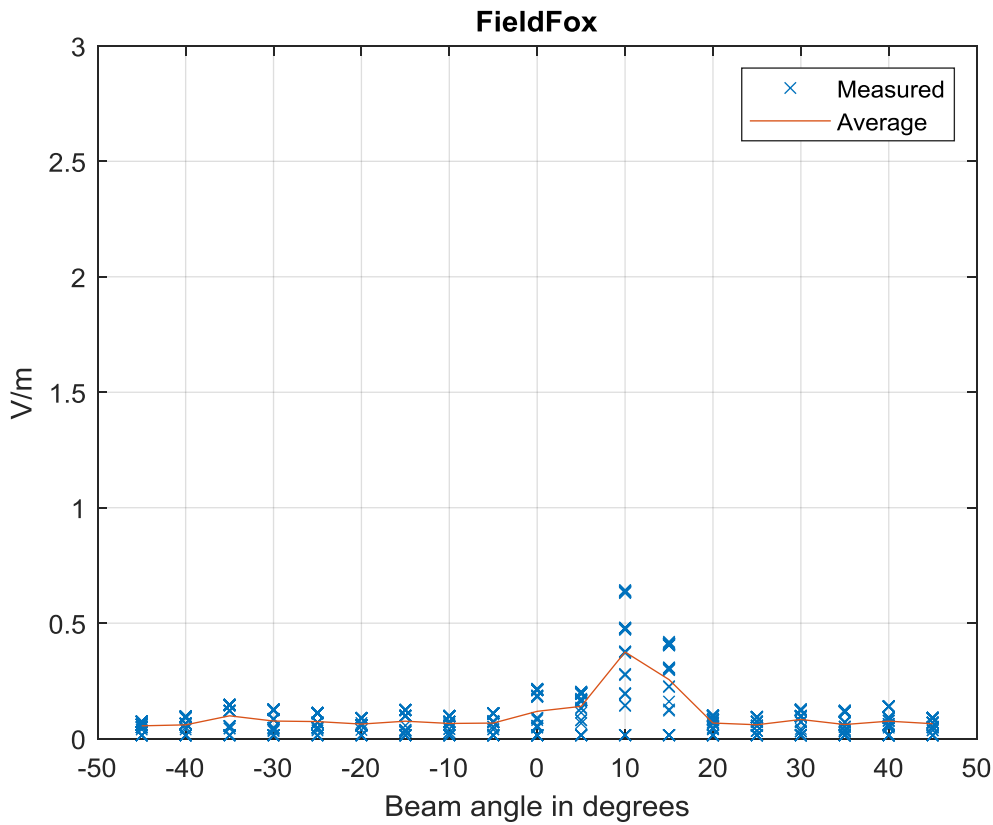
3.2.2 Findings

To understand the statistical variation of the RF-exposure (in V/m) as a function of the number of users in the system, by using the number of beams as proxy (i.e. assuming that each beam is steered towards a given user), Figure 14 depicts the empirical calibrated RF-exposure and their cumulative distribution function (CDF) based on the FieldFox measurements. More precisely, Figure 14(a) depicts the RF-exposure values measured by the FieldFox when only 1 beam was active and steered in the direction indicated by the x-axis, where each blue cross represents one measurement and the orange curve is the averaged RF-exposure of all the measurements.

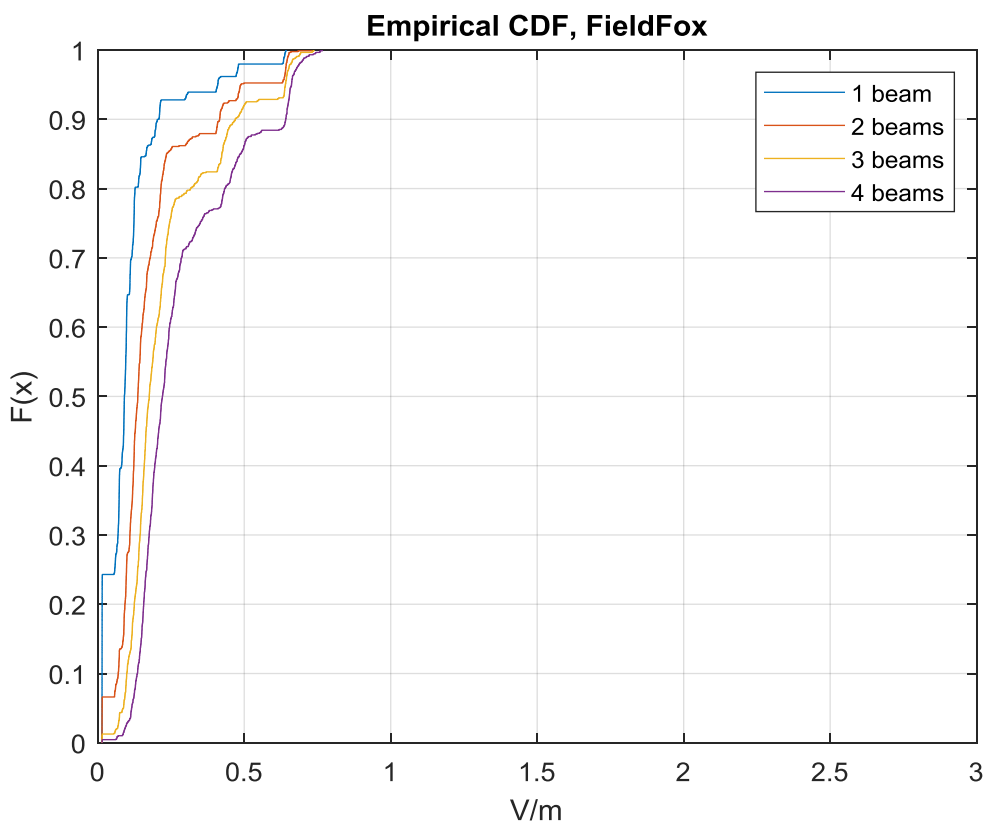
The results clearly indicates that the maximum of the exposure is reached in the direction of P1, which is according to Figure 13 around 11 degree. In other words, if the FieldFox was a user or a bystander at position (1 m, 5 m) then its exposure could be up to 7 times higher when a beam is steered in its direction compared to if its steered away from it. Meanwhile, Figure 14(b) depict the empirical CDF of the RF-exposure when one, two, three or four beams are simultaneously active. The results clearly indicate that the more beams are active, the more RF-exposure is generated towards the probe.

The increases in exposure seems to be linear with the number of active beams. To confirm the probe measurements, Figure 15 and Figure 16 depict, respectively the empirical calibrated RF-exposure and their CDF of the five other receivers. It shows that more exposure occurs when the beam is steered in the general direction of the receiver and that more beams/users imply a higher exposure. It also shows that the closer the receivers are from the BS, the higher the exposure they experienced, especially when a beam is steered towards them.

Overall, the exposure at a given point increases with the number of users that are served (equivalently, the number of beams that are used) simultaneously by the mMIMO BS. This is interesting because this somehow contradicts one insight gained from Figure 12 in the first experiment. This is likely due to the fact that the number of measurements in Figure 12 were not large enough to be statistically meaningful. The rate of increase seems to be more or less linear with the number of users in certain cases and more experiments will be required to get a definitive answer on this.



(a)



(b)

Figure 14 The empirical calibrated RF-exposure results of the FieldFox probe (P1) (a) for 1 active beam as a function of the beam angle; (b) empirical cdf of the RF-exposure for 1 to 4 active beams.

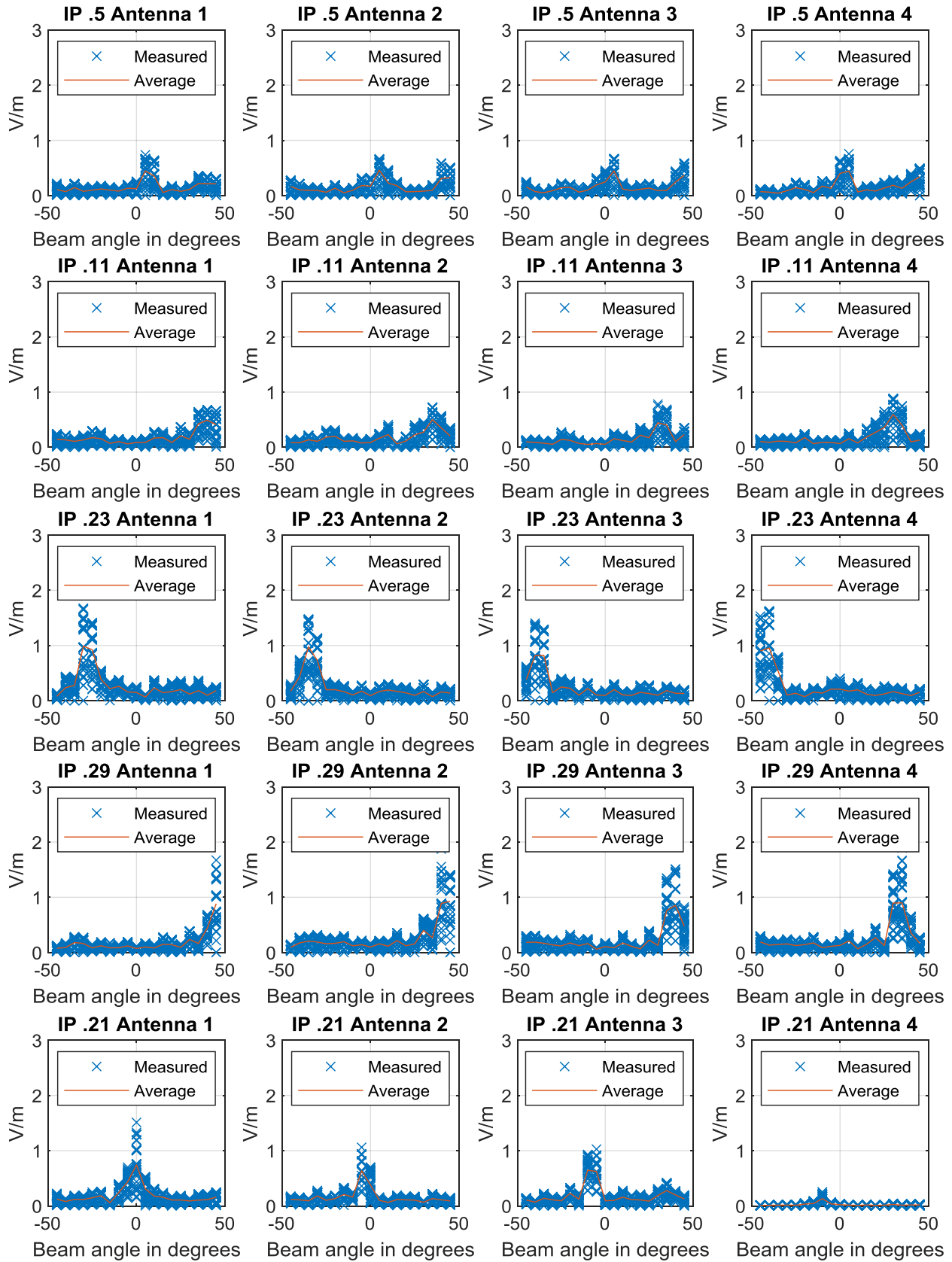


Figure 15 The empirical calibrated RF-exposure results of the four antennas of the five receivers (Rx3, Rx5, Rx1, Rx4, Rx2) for 1 active beam as a function of the beam angle.

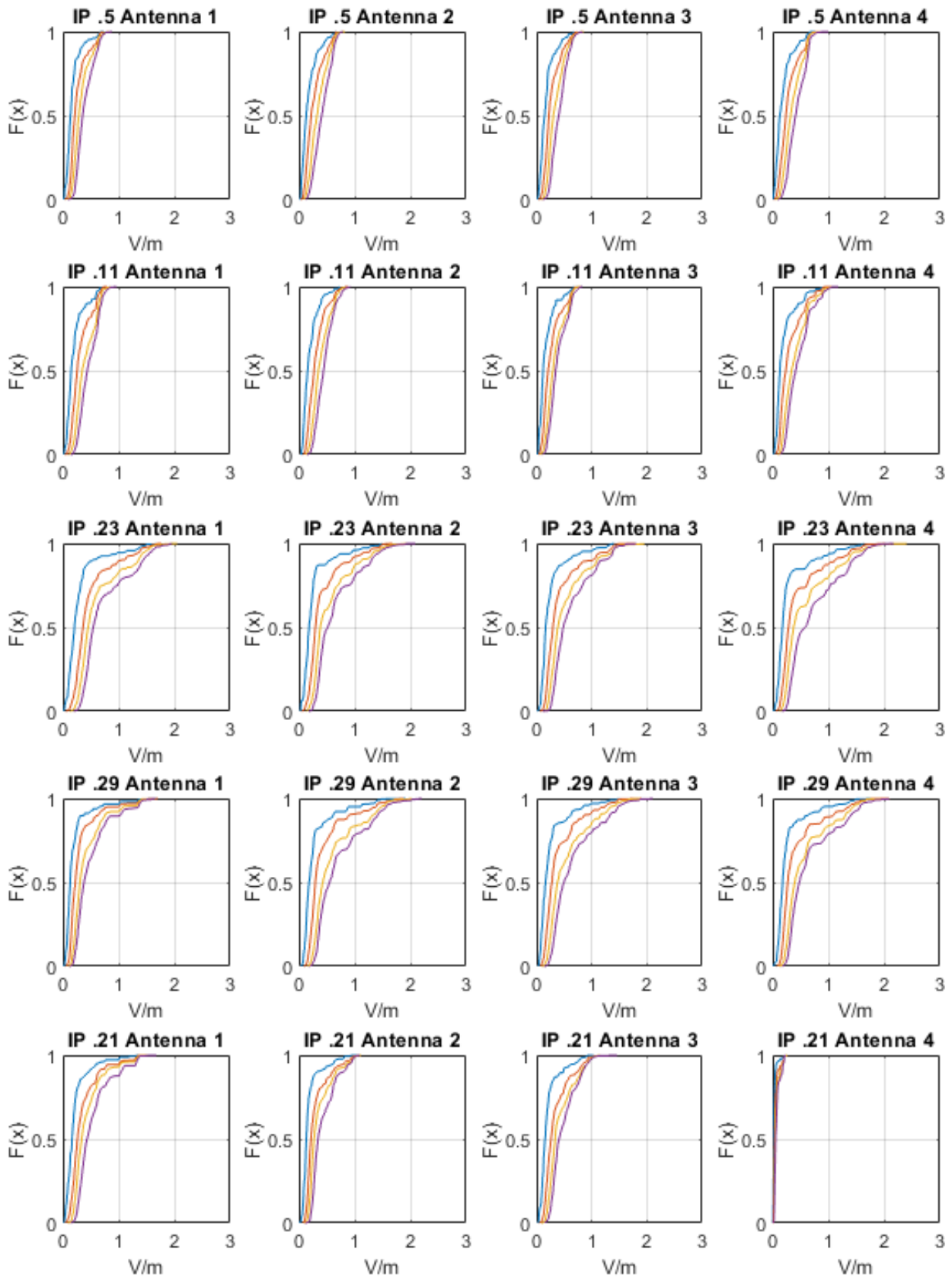


Figure 16 *The empirical calibrated RF-exposure results of the four antennas of the five receivers (Rx3, Rx5, Rx1, Rx4, Rx2) for empirical cdf of the RF-exposure for 1 to 4 active beams, coloured blue, red, yellow, and purple respectively.*

3.3 Indoor Measurement Campaign (3)

In this indoor measurement campaign, the measurement system was setup to compare the two RF-EMF measurement methods, namely, the field strength method and the SSB based method (see Deliverable Report D2 for further details).

3.3.1 Measurement setup and test scenarios

A spacious meeting room was chosen in the 5GIC at the University of Surrey for carrying out this measurement campaign. The mMIMO system located at (0 m, 0 m) within the room acts as the 5G BS Tx system of which 96 antennas were activated where the Keysight field probe RF-EMF measurement system is located at (0 m, 4 m) within the room (see

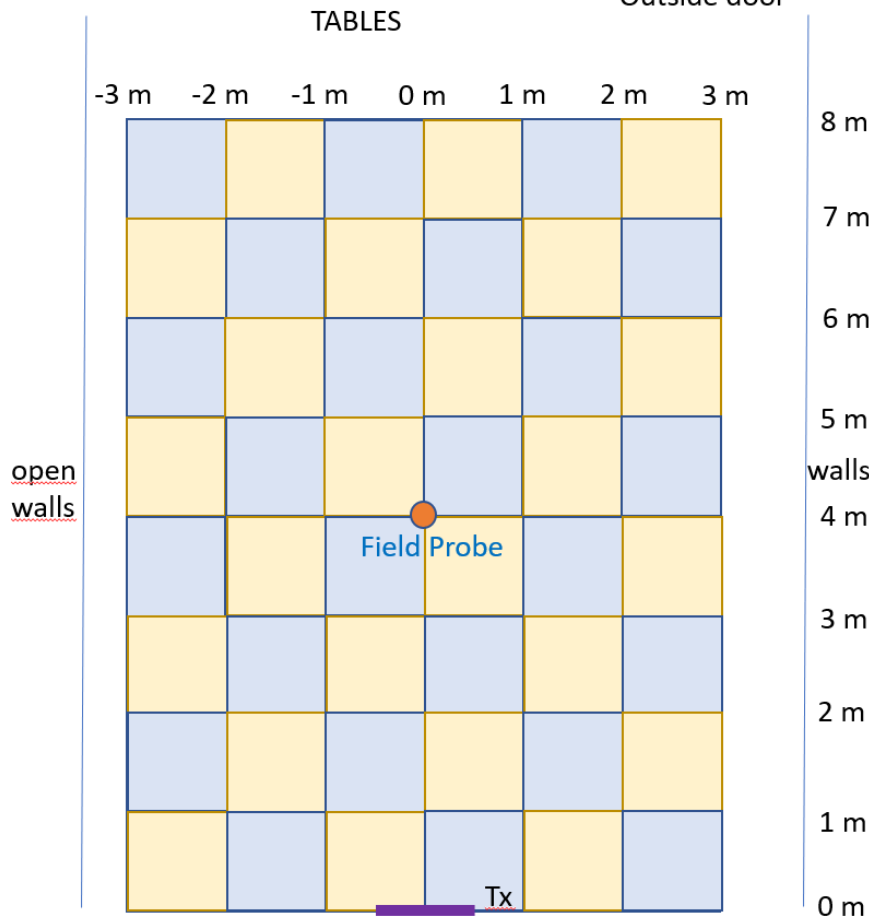


Figure 17). i.e. the Keysight RF-exposure measurement probe was located at the boresight of the mMIMO Tx antenna array.

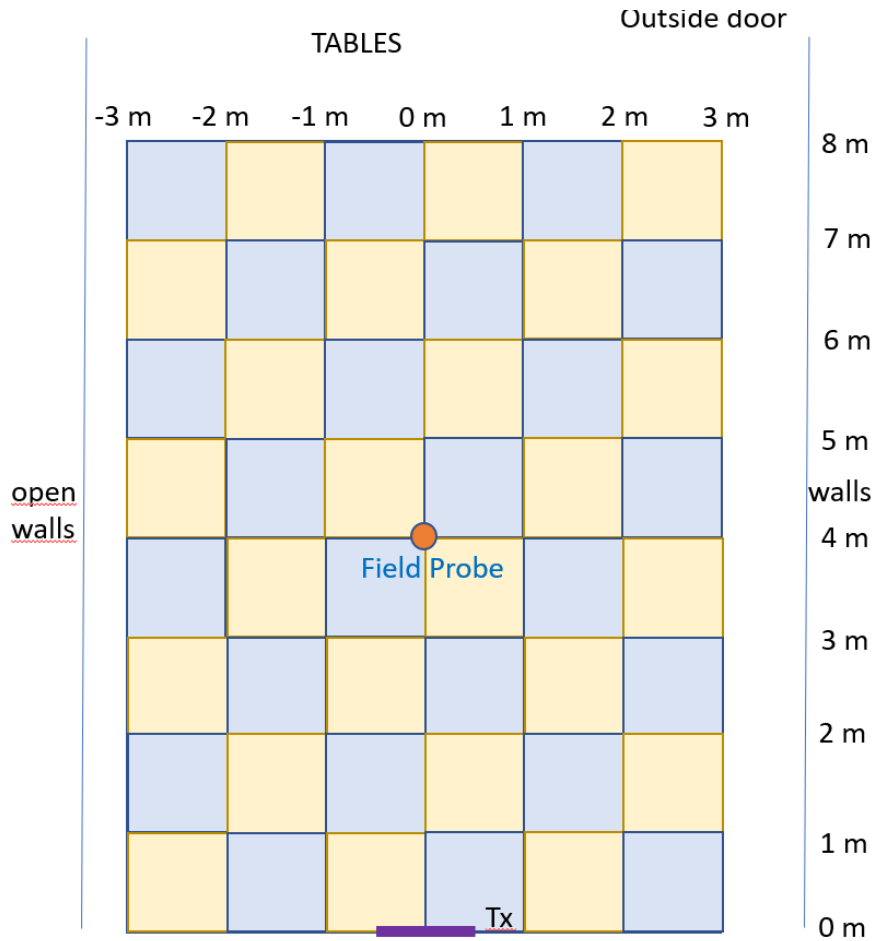


Figure 17 Measurement setup for comparison between the two RF-EMF measurement methods. Note that mMIMO Tx system is located at (0 m, 0 m) and the Keysight RF-EMF field probe are located at (0 m, 4 m) within the room.

For the field strength RF-EMF method, the mMIMO Tx system was setup to operate similar to the measurement setting in Section 3.2 with random active beams, payload data rate and non-normalized transmit power. For the SSB based RF-EMF method, the mMIMO Tx system was setup to generate the SSB broadcasting signal according to 3GPP 5G NR protocol where the transmitted SSB signal was continuous repeated and the transmitted power is normalized. In order to compare these RF-EMF methods, the mMIMO Tx system while operating with SSB based RF-EMF method, was setup to sweep in all the 19 potential beam directions that is equally spaced every 5° between $\pm 45^\circ$ in azimuth and elevation= 0° . i.e. the same beam direction setup as for the field strength RF-EMF method. To avoid complexity only one beam is activated at a time.

3.3.2 Findings

The Figure 18 and Figure 19 show the relevant RF-EMF distribution according to the swept beam directions by using field strength method and SSB based method, respectively. The orange line in Figure 18 show the average of the acquired RF-EMF measurements for randomly chosen data rates at each swept beam direction. The result of the SSB based method shown in Figure 19 is achieved by measuring the RSRP of SS Block resource element, extrapolating by using the factors $F_{PR} = 1$, $F_{TDC} = 1$, and $F_{BW} = 2592$ according IEC's SSB method equation IEC 62232 F.9.2.1.2.

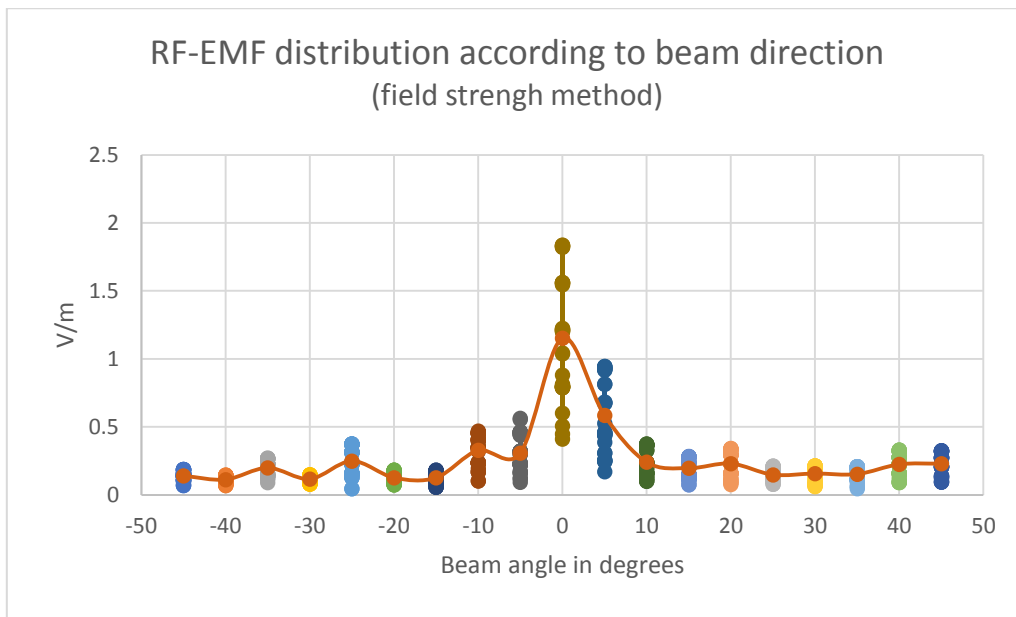
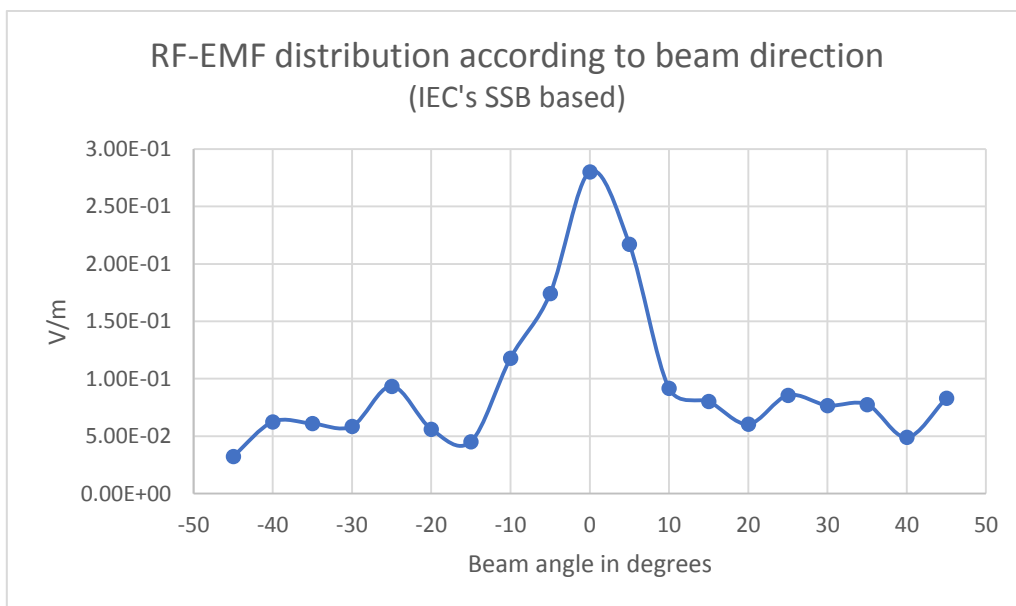


Figure 18 RF-EMF distribution according to beam direction by using field strength method. Note: the orange line shows the average of the measured results.



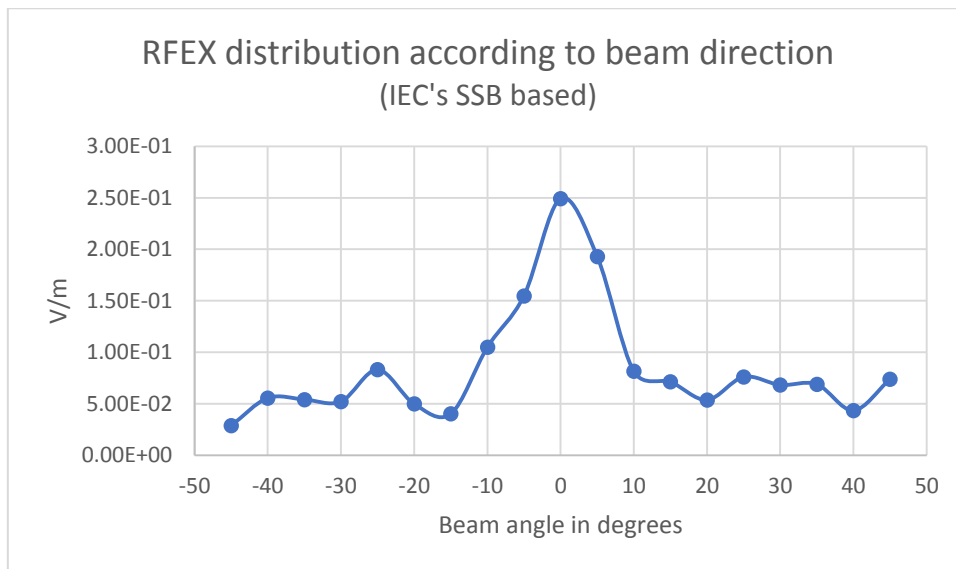


Figure 19 RF-EMF distribution according to beam direction by using IEC's SSB based method.

From these results, the peak at 0° direction is envisaged as the Keysight field probe was located at 0° direction from the mMIMO system. i.e. strong signal should be detected by the probe which is located at the boresight direction when the main beam of mMIMO BS Tx system is pointing towards it. Note that there is no reflector in proximity between the mMIMO BS Tx system and the measurement probe within the room. By comparing both Figure 18 and Figure 19, one observes very similar distribution pattern between these RF-EMF methods. The difference in the RF-EMF between the two methods is envisaged due to the fact that the transmitted power for field strength based method is not normalized whereby the transmitted power for the SSB based method is normalized. i.e. there is existing difference of the transmission reference power when conducting the two measurement methods. Nevertheless, one envisages that the SSB based method could be used to evaluate the RF-EMF level without going through vast data rate samples as the field strength method.

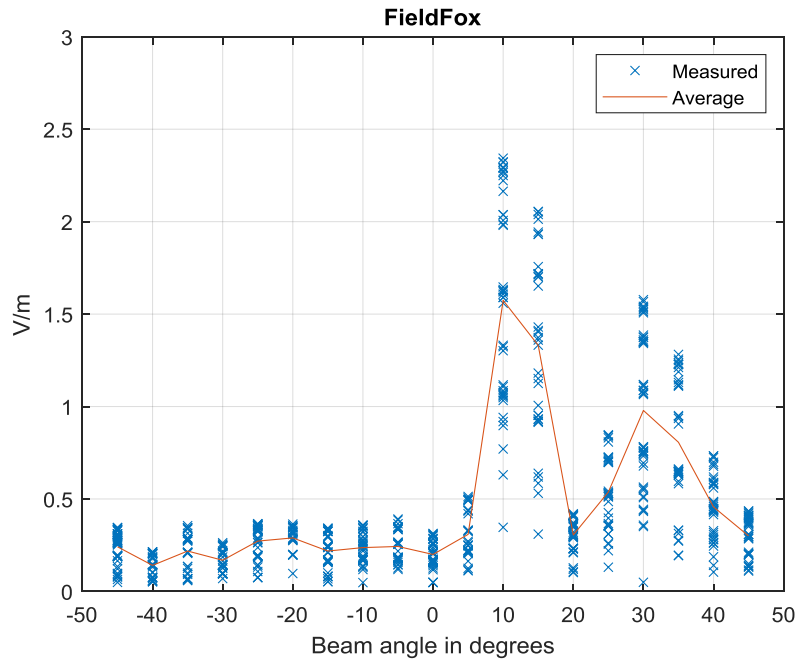
4 Outdoor Measurement Campaign with mMIMO testbed

4.1 Outdoor Measurement Campaign (1)

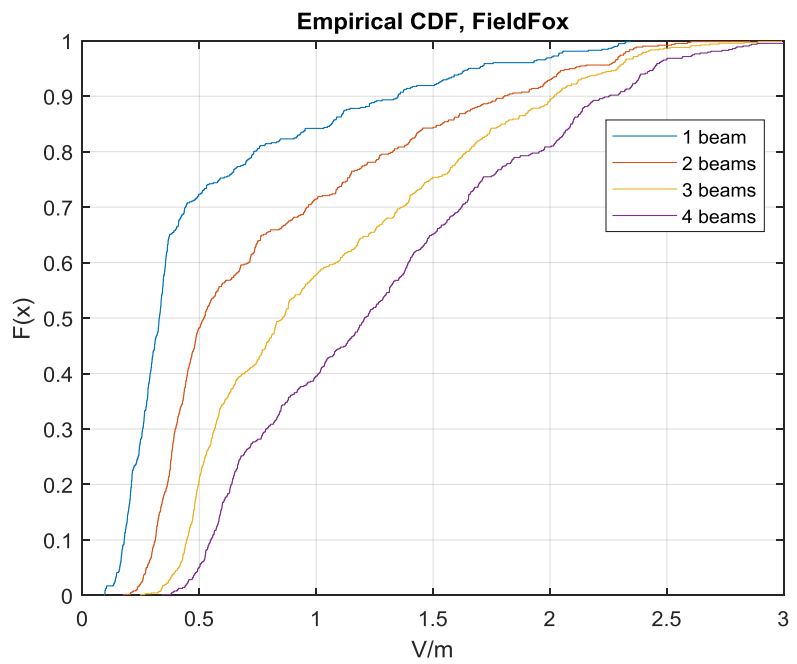
The measurement process used for the indoor measurements in Section 3.2 was repeated in an outdoor scenario where a photograph of the measurement setup is shown in Figure 20.

4.1.2 Findings

Figure 22(a) and Figure 23 show the RF-EMF measurement results for the mMIMO testbed system operating with only one activated beam, which was filtered from all the acquired E-field measurement results. The results show that in this outdoor scenario more than one beams are detected by some of the receivers, i.e. RF-EMF peaks at more than one transmitted angle. Especially for those in proximity to an object. A possible explanation for this might be that one of the peaks shown in the measurement E-field results is caused by the direct LOS propagation path between the mMIMO Tx and RF-EMF Rx systems and that the second peak is caused by an indirect propagation path reflecting off an object in close proximity. A likely source of this in this scenario is the window adjacent to the measurement location as shown in Figure 20.



(a)



(b)

Figure 22 The empirical calibrated RF-exposure results of the FieldFox probe (P1) in the Surrey outdoor measurement campaign: (a) for 1 active beam as a function of the beam angle; (b) empirical

CDF of the RF-exposure for 1 to 4 active beams.

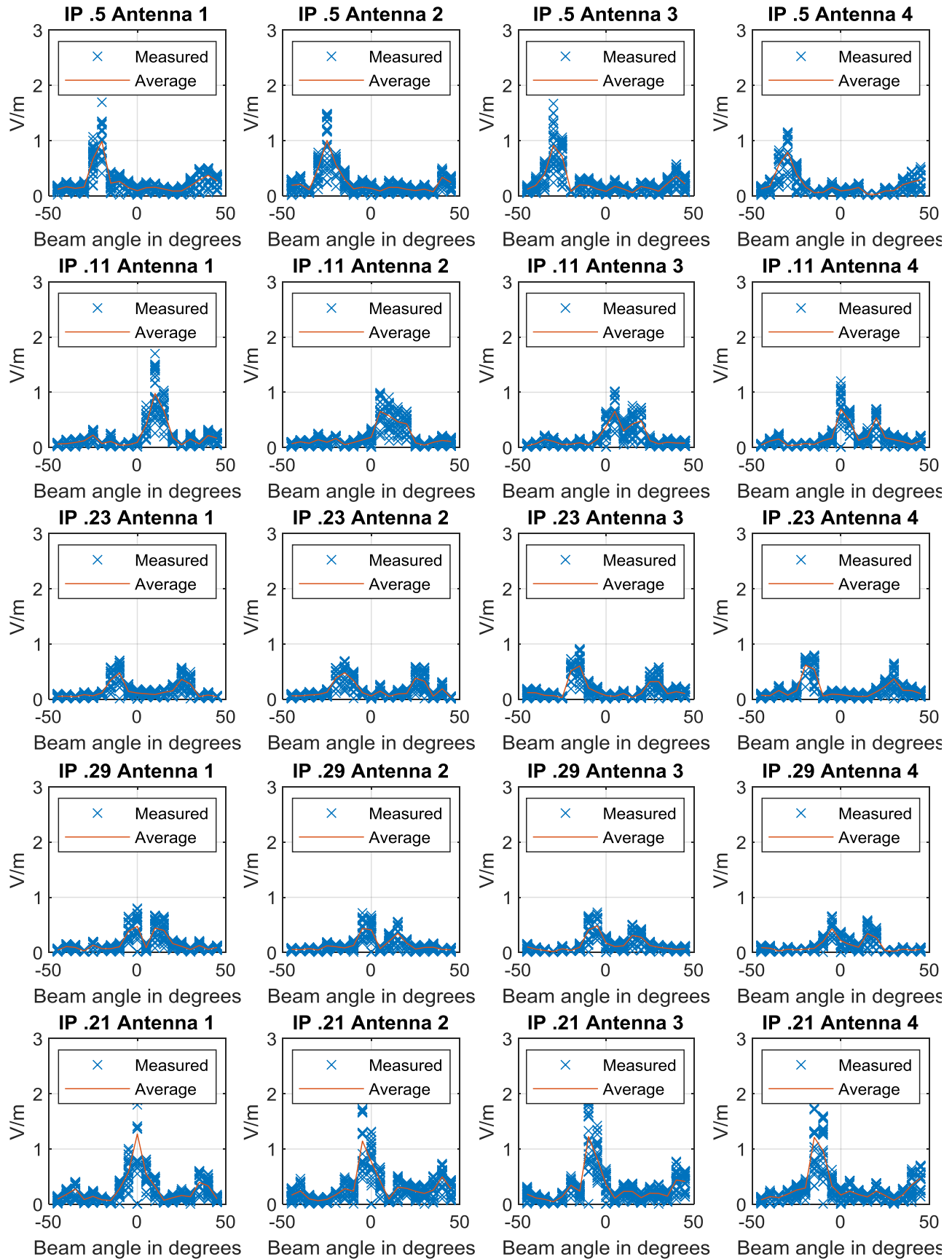


Figure 23 *The empirical calibrated RF-exposure results of the four antennas of the five receivers (Rx3, Rx5, Rx1, Rx4, Rx2) in outdoor scenario for 1 active beam as a function of the beam angle.*

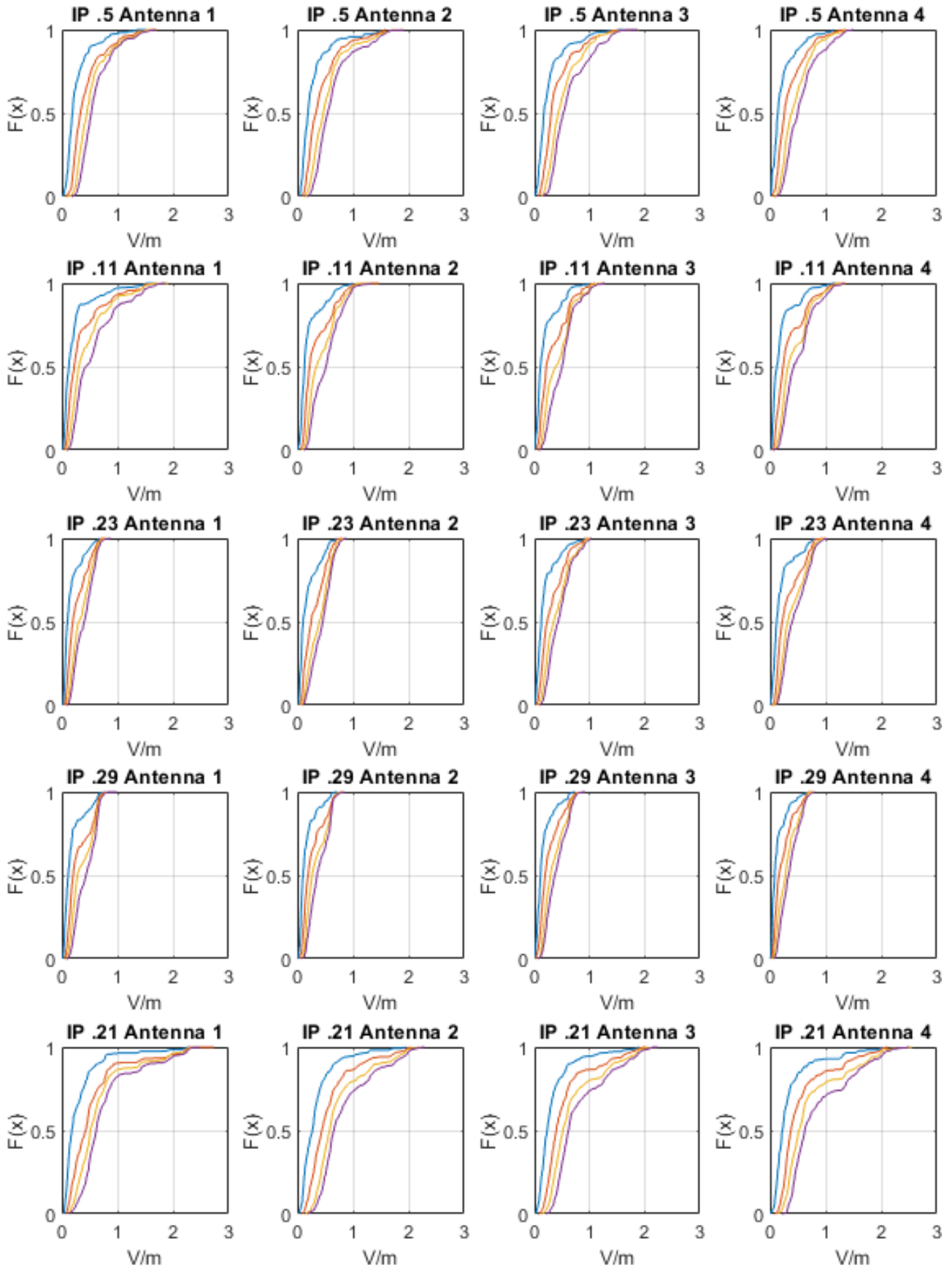


Figure 24 The empirical calibrated RF-exposure results of the four antennas of the five receivers (Rx3, Rx5, Rx1, Rx4, Rx2) in outdoor scenario for empirical cdf of the RF-exposure for 1 to 4 active

beams, coloured blue, red, yellow, and purple respectively.

Figure 22(b) and Figure 24 depict the empirical CDF of the RF-EMF measurement results based on all measurements and at the five receivers, respectively, when one, two, three or four beams are simultaneously active. Similar to the findings in Section 4, the results clearly indicate that the more beams are active, the higher RF-exposure is generated towards the probe and the receiver. Overall, the exposure at a given point increases with the number of active beams simultaneously by the mMIMO BS.

Figure 25, Figure 26, and Figure 27 show, respectively, the further statistical analysis on how the measured RF-EMF are affected by the number of active beams, number of active transmit antennas, and the total number of used resource blocks. Both the measured E-field results and their average are plotted. From these results, one observes that the average RF-EMF exposure generally increases with these factors.

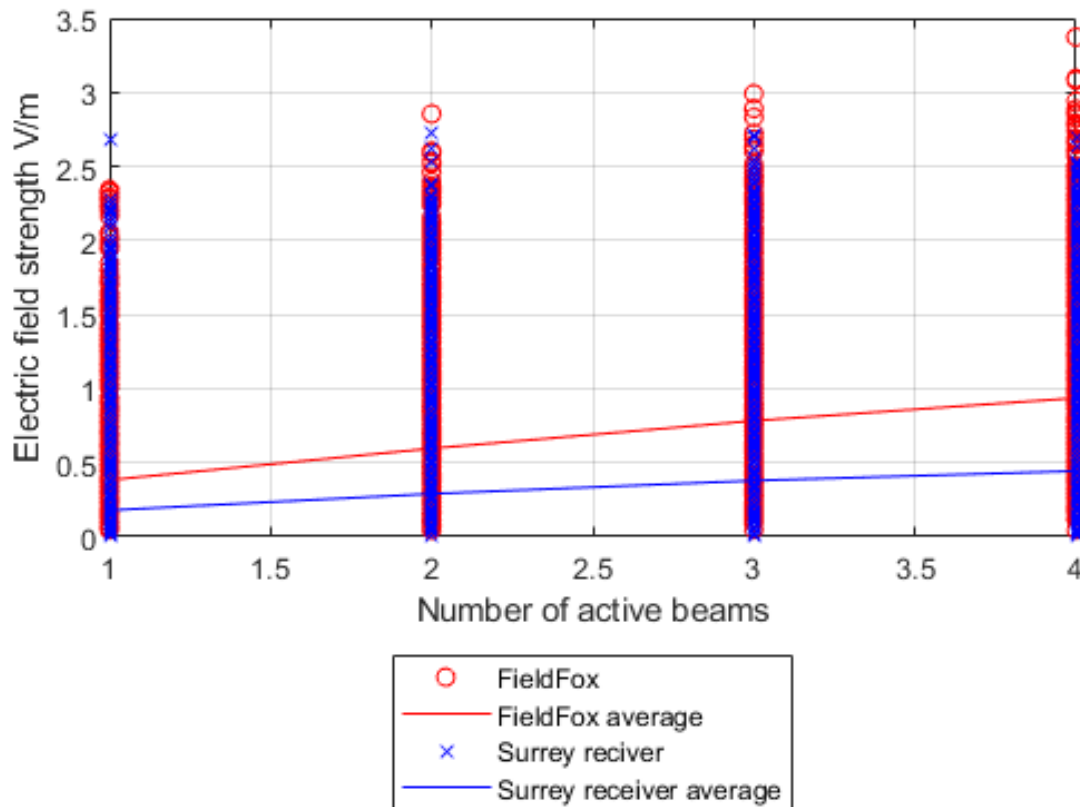


Figure 25 Plot of the calibrated E-field measurement results and their average for different number of active beams.

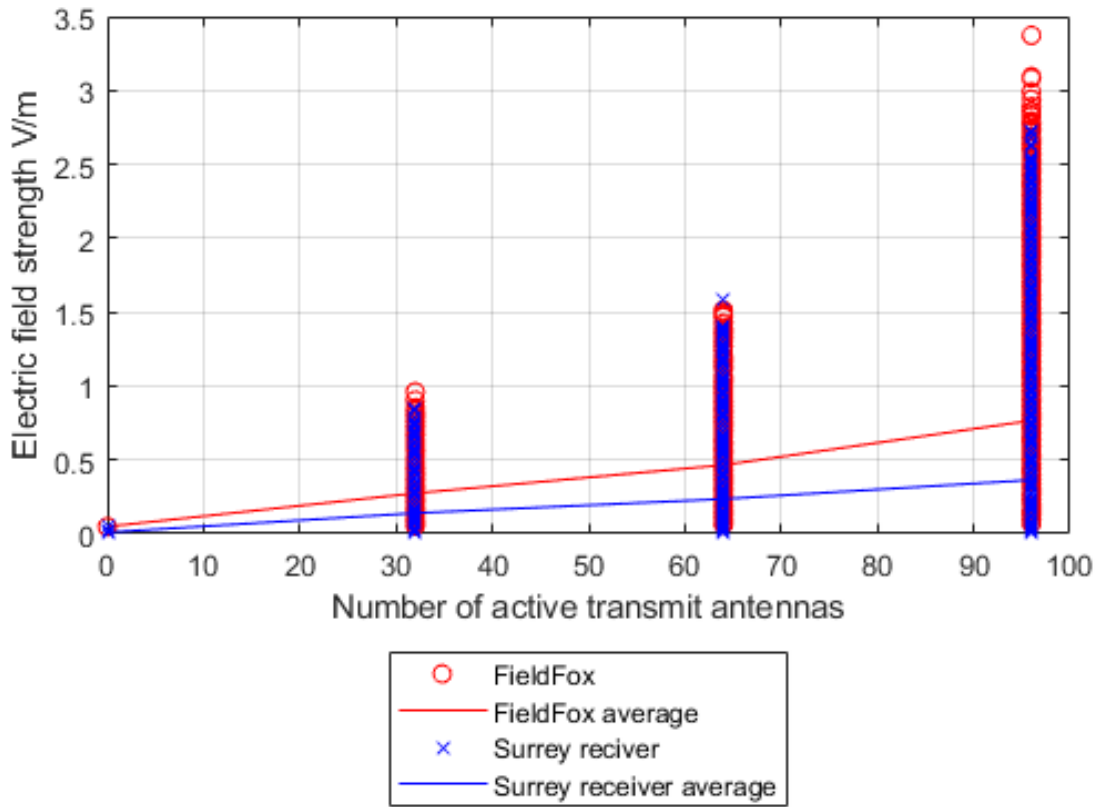


Figure 26 Plot of the calibrated E-field measurement results and their average for different number of active transmit antennas.

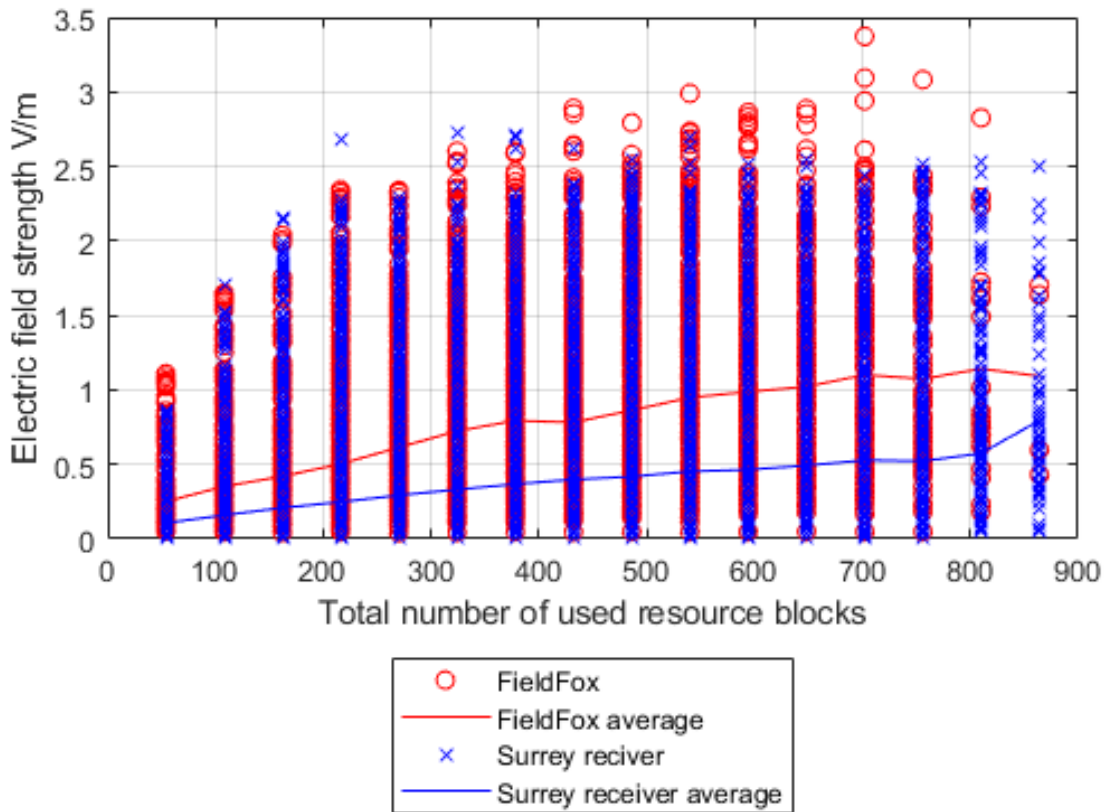


Figure 27 Plot of the calibrated E-field measurement results and their average for different total number of used resource blocks.

4.2 Outdoor Measurement Campaign (2)

In the scenario, we arrange an outdoor measurement campaign to compare the two measurement methods, the field strength method and the SSB based method.

4.2.1 Measurement setup and test scenarios

A similar scenario with outdoor measurement campaign (1) has been chosen in this section whereby additional measurement samples for Surrey RF-EMF receivers located at different locations and heights have also been considered. The RF-exposure measurement probe was located at the direction 10° offset from the boresight of the Tx antenna array as shown in Figure 28.



Figure 28 *Photograph of the experimental setup for the outdoor RF-EMF measurement campaign (2) for comparison between the two RF-EMF methods.*

For the field strength RF-EMF method, the mMIMO Tx system was setup to operate similar to the measurement setting in Section 3.2 with random active beams, payload data rate and non-normalized transmit power. For the SSB based RF-EMF method, the mMIMO Tx system was setup to generate the SSB broadcasting signal according to 3GPP 5G NR protocol where the transmitted SSB signal was continuous repeated and the transmitted power is normalized. Similar to Section 3.3, in order to compare these RF-EMF methods, the mMIMO Tx system while operating with SSB based RF-EMF method, was setup to sweep in all the 19 potential beam directions that is equally spaced every 5° between $\pm 45^\circ$ in azimuth and elevation= 0° . i.e. the same beam direction setup as for the field strength RF-EMF method. To avoid complexity only one beam is activated at a time.

4.2.2 Findings

The Figure 29 and Figure 30 show the relevant RF-EMF distribution according to the swept beam directions by using field strength method and SSB based method, respectively. The orange line in Figure 29 show the average of the acquired RF-EMF measurements for randomly chosen data rates at each swept beam direction. The result of the SSB based method shown in Figure 30 is achieved by measuring the RSRP of SS Block resource element, extrapolating by using the factors $F_{PR} = 1$, $F_{TDC} = 1$, and $F_{BW} = 2592$ according IEC's SSB method equation IEC 62232 F.9.2.1.2.

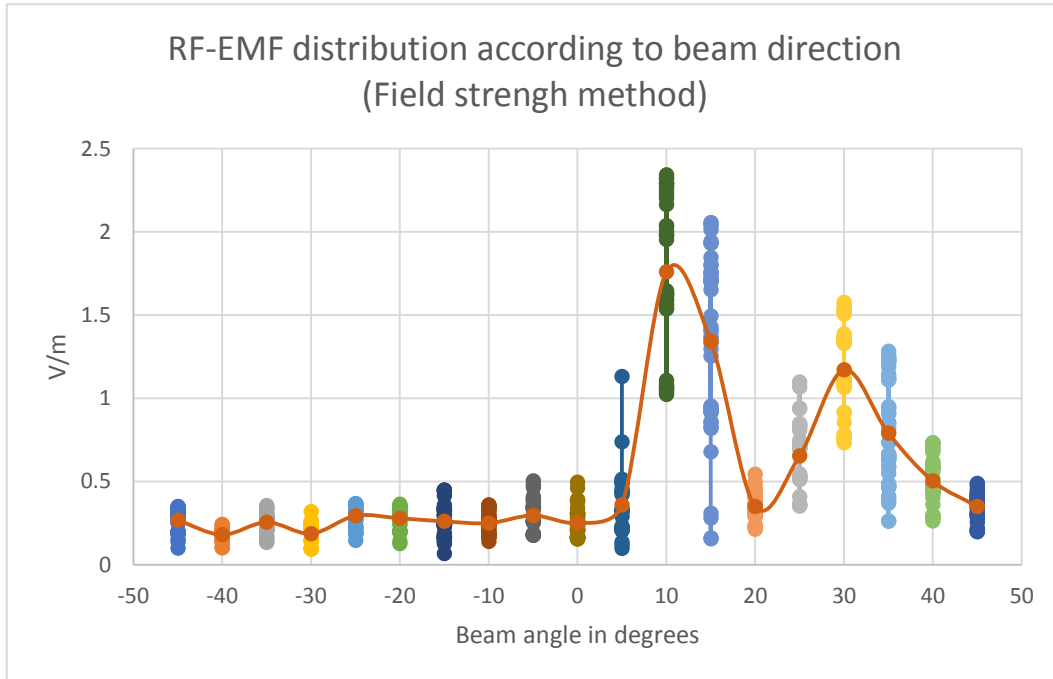


Figure 29 RF-EMF distribution according to beam direction by using field strength method. Note: the orange line shows the average of the measured results.

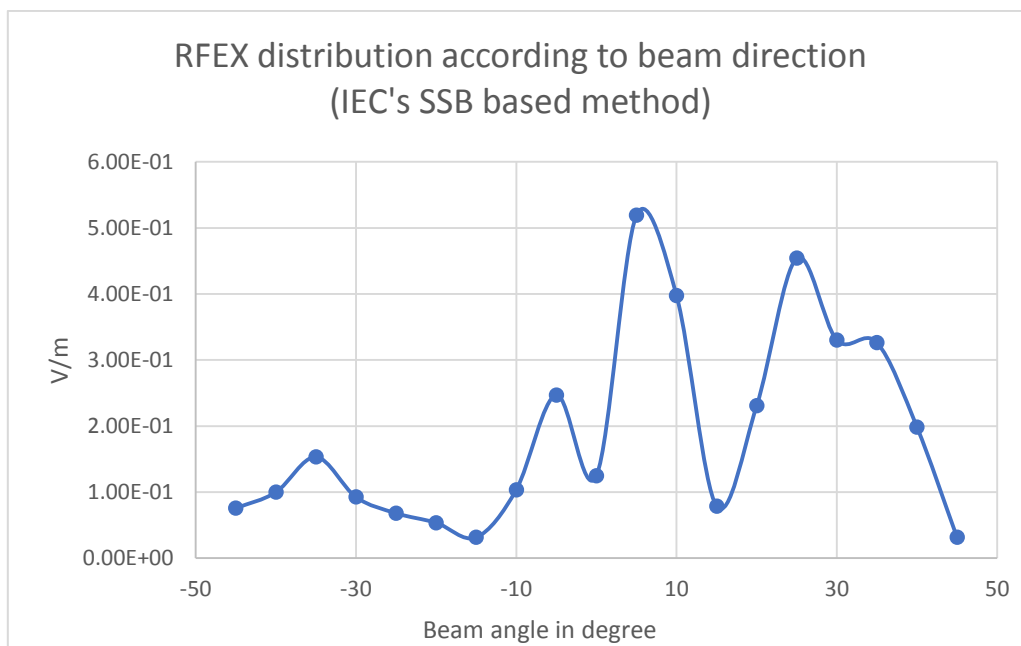
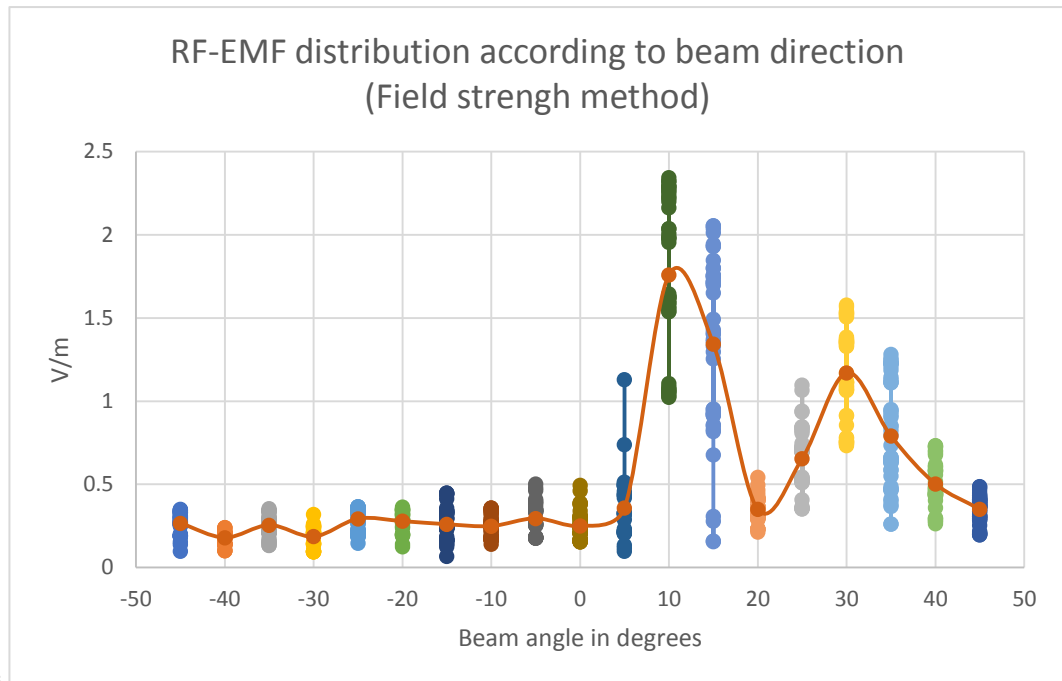


Figure 30 RF-EMF distribution according to beam direction by using IEC's SSB based method.



As shown in the

, a peak could be observed at 10° direction, which is envisaged as the Keysight field probe was located at 10° direction from the mMIMO system. i.e. strong LOS path signal should be detected by the probe which is located at the 10° direction when the main beam of mMIMO BS Tx system is pointing towards it. However, two other ‘undesired’ peaks could also be observed in the 30° and -10° directions due to the nearby reflectors (i.e. the window) around the probe.

By comparing both Figure 29 and Figure 30, one observes very similar distribution pattern between these RF-EMF methods. The difference in the RF-EMF between the two methods is envisaged due to the fact that the transmitted power for field strength based method is not normalized whereby the transmitted power for the SSB based method is normalized. i.e. there is existing difference of the transmission reference power when conducting the two measurement methods. Nevertheless, one envisages that the SSB based method could be used to evaluate the RF-EMF level without going through vast data rate samples as the field strength method.

5 Outdoor RF-EMF Measurement Campaign of 5G base station

An experimental work has been carried out for RF-EMF assessment of a 5G BS in an outdoor environment. During the measurement campaigns various varying factors such as number of users, position of users and data duty cycles have been considered. The following sub-sections provides the details of the measurement setup, test scenarios and some findings.

5.1 Measurement setup and test scenarios

The experimental work for RF-EMF assessment of a 5G BS in an outdoor environment was enabled through access to the test infrastructure provided by project 5G-VINNI (H2020 N° 815279) [13]. The measurement campaign has been carried out at the 5G-VINNI UK facility, based at British Telecom (BT)’s Adastral Park, Ipswich. During the measurement campaign, all other 5G-VINNI 4G and 5G BSs have been turned off so to avoid potential interferences. Figure 31 shows the illustrative Google map view of the test site within the Adastral Park site. As depicted in the map shown in Figure 31, the 5G BS is located at the top of the multi-storey building at the southern part within the test area. The test area of which the envisaged active beam(s) of the 5G BS being covered includes the car park

area and the grassland with rich woods. A double-storey restaurant, with a mixed façade of glass and concrete, is located just behind the woods.



Figure 31 Measurement setup for the RF-EMF assessment of a commercial 5G BS in an outdoor environment at UK BT Adastral Park site in Ipswich. Note that the distance of each UE from the BS is marked at the UE.

Five Samsung 5G mobile phones (also refer to as user equipment (UE)) were employed as test terminals for stimulating the demand on downlink data transmission. As shown in Figure 31, these UEs are placed in five fixed locations, respectively, which are distributed across the trial field area. Their locations take account over the line of sight (LoS) scenarios at open area and the non-line-of-sight (NLoS) scenarios (e.g. indirect path scene blocked by trees).

Among them, UE1 and UE2 are located at both ends of the car park area operating as LoS scenarios, although compared with UE1, UE2 is situated nearer the centre of the trial field. UE3 is located around the centre of the trial field along the road leading toward the BS. UE4 is farthest from the BS among the 5 UEs, at the restaurant entrance, just at the edge of the woods. UE5 is located at the edge of the trial field and at the far eastern edge of the wood.

In this measurement campaign, the Keysight RF-EMF measurement system has been employed for RF-EMF exposure measurement. The probe can simultaneously measure the RF exposure in x -, y - and z -axes. The field probe is located in an open area near UE2 (LoS from Basestation), and the probe position remains unchanged throughout the whole measurement procedure. Figure 32 to Figure 36 show the measurement setup photos for UE1 to UE5, respectively.



Figure 32 Measurement setup for UE1 at the UK 5G-VINNI 5G BS in an outdoor environment.



Figure 33 Measurement setup for UE2 and the Keysight RF-EMF measurement system for the assessment of the UK 5G-VINNI 5G BS in an outdoor environment.



Figure 34 *Measurement setup for UE3 at the UK 5G-VINNI 5G BS in an outdoor environment.*



Figure 35 Measurement setup for UE4 at the UK 5G-VINNI 5G BS in an outdoor environment.



Figure 36 *Measurement setup for UE5 at the UK 5G-VINNI 5G BS in an outdoor environment.*

An App entitled ‘iPerf’ is used in each UE terminal for connection to the 5G BS (see Figure 37). Different data rates could be configured by setting appropriate parameters in the commander script.



Figure 37 Measurement setup for the RF-EMF assessment of the UK BT 5G BS in an outdoor environment.

In this measurement campaign, three targetted data rate levels setting at the UE terminal are chosen, namely, ‘High’ (i.e. UE targeted data rate set to 100%), ‘Medium’ (i.e. UE targeted data rate set to 50%) and ‘Low’ (i.e. UE targeted data rate set to 10%). The envisaged data rate achieved at each UE terminal will depend on its targeted data rate level and the number of activated UEs. Table 1 shows the envisaged data rate achieved at each UE terminal for various combination of the number of activated UE(s) and its targeted data rate level. In practice, the actual data rate also depends on the quality of the wireless channel link between the BS and the relevant UE. Table 4 shows the test cases for the RF-EMF assessment of the UK 5G-VINNI 5G BS in an outdoor environment.

Table 3 Envisage data rate achieved at each UE terminal.

| | | |
|-------------|--------|---------|
| Single User | High | 700MB/s |
| | Medium | 350MB/s |
| | Low | 70MB/s |
| Two Users | High | 350MB/s |
| | Medium | 230MB/s |
| | Low | 35MB/s |
| Three Users | High | 230MB/s |
| | Medium | 120MB/s |
| | Low | 30MB/s |
| Four Users | High | 180MB/s |
| | Medium | 90MB/s |
| | Low | 30MB/s |
| Five Users | High | 120MB/s |
| | Medium | 60MB/s |
| | Low | 30MB/s |

Table 4 Test cases for the RF-EMF assessment of the UK 5G-VINNI 5G BS in an outdoor environment.

| | | | |
|-------------|-----------|--------|---------|
| Single User | UE1 | High | 700MB/s |
| | | Medium | 350MB/s |
| | | Low | 70MB/s |
| | UE2 | High | 700MB/s |
| | | Medium | 350MB/s |
| | | Low | 70MB/s |
| | UE3 | High | 700MB/s |
| | | Medium | 350MB/s |
| | | Low | 70MB/s |
| | UE4 | High | 700MB/s |
| | | Medium | 350MB/s |
| | | Low | 70MB/s |
| | UE5 | High | 700MB/s |
| | | Medium | 350MB/s |
| | | Low | 70MB/s |
| Two Users | UE1 & UE2 | High | 350MB/s |

| | | | |
|-----------------|-----------------------------|---------|---------|
| | | Medium | 230MB/s |
| | | Low | 35MB/s |
| | UE1 & UE5 | High | 350MB/s |
| | | Medium | 230MB/s |
| | | Low | 35MB/s |
| | UE2 & UE4 | High | 350MB/s |
| | | Medium | 230MB/s |
| | | Low | 35MB/s |
| | UE2 & UE3 | High | 350MB/s |
| Medium | | 230MB/s | |
| Low | | 35MB/s | |
| Three Users | UE1 & UE3 & UE5 | High | 230MB/s |
| | | Medium | 120MB/s |
| | | Low | 30MB/s |
| | UE2 & UE3 & UE4 | High | 230MB/s |
| | | Medium | 120MB/s |
| | | Low | 30MB/s |
| UE1 & UE2 & UE3 | High | 230MB/s | |
| | High | 230MB/s | |
| Four Users | UE1 & UE2 & UE3 & UE4 | High | 180MB/s |
| | | Medium | 90MB/s |
| | | Low | 30MB/s |
| | UE1 & UE2 & UE4 & UE5 | High | 180MB/s |
| Five Users | UE1 & UE2 & UE3 & UE4 & UE5 | High | 120MB/s |
| | | Low | 30MB/s |

5.2 Findings

The following table shows the probability distribution (i.e. histogram) of RF-EMF exposure levels based on the collection of all the measurement configurations, including all active terminal numbers, and all active terminal patterns, and all different transmission rates of the active terminals. The most likelihood RF-EMF exposure level is around 1.34 V/m.

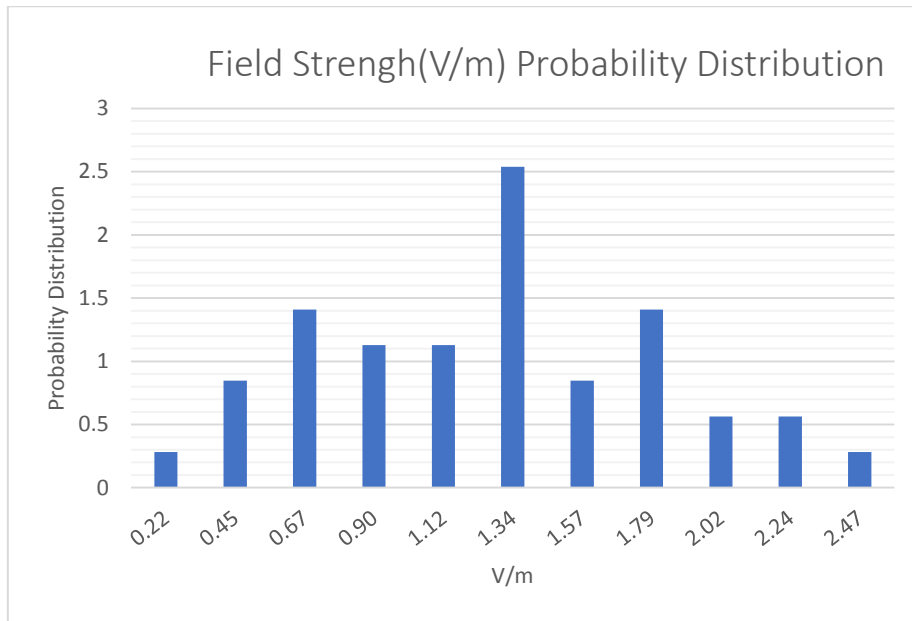


Figure 38 Probability distribution (i.e. Histogram) of RF-EMF exposure levels based on all measurements.

Figure 39 to Figure 41, respectively, show the impact on RF-EMF exposure level due to the active UE numbers, data rates and relative UE position from the measurement probe (for single user test cases). Figure 39 shows similar CDF variation for different number of activated UEs. The reason is believed due to the available total resource blocks at BS while active is fixed, i.e. the total data rate holds invariability regardless how many active UEs.

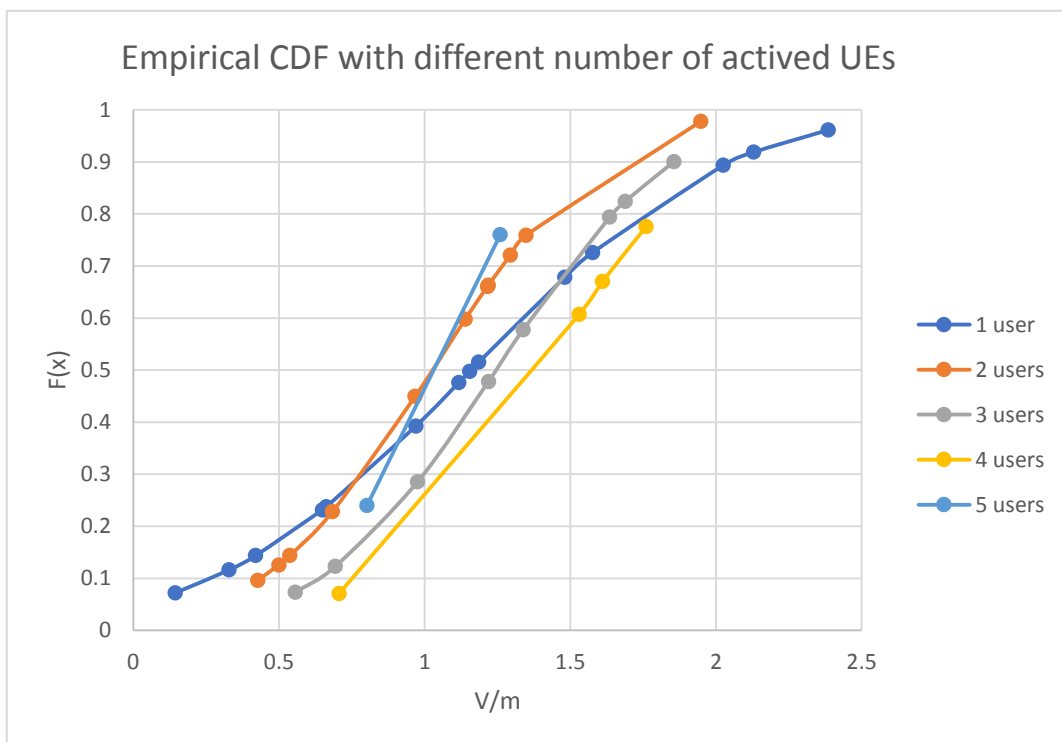


Figure 39 CDF of RF-EMF exposure levels based on number of activated UE(s).

Figure 40 shows the CDF of RF-EMF exposure level increases as the average users' data rate increases. That is, regardless of the number of active users, when the overall active user data rate increases, the RF-EMF exposure level will increase simultaneously.

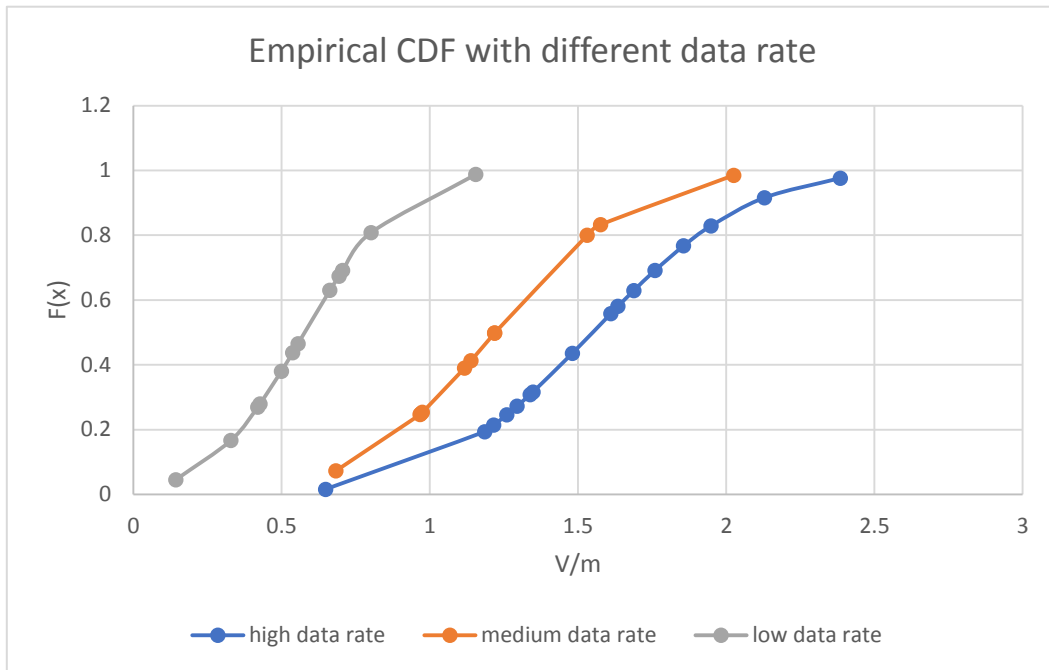


Figure 40 CDF of RF-EMF exposure levels based on data rates.

Figure 41 shows the empirical RF-EMF exposure levels acquired at the probe when only one of the UE terminal is active at a time. For different UE terminal positions, the BS will generate corresponding beam directions. In theory, the closer these beams are aligned with the direction pointing towards the probe from the BS, the larger affect is envisaged towards the measured RF-EMF exposure level. However, one observes from the results for single user test cases that the RF-EMF exposure level is also affected by the distance of the active UE location from the RF-EMF measurement probe.

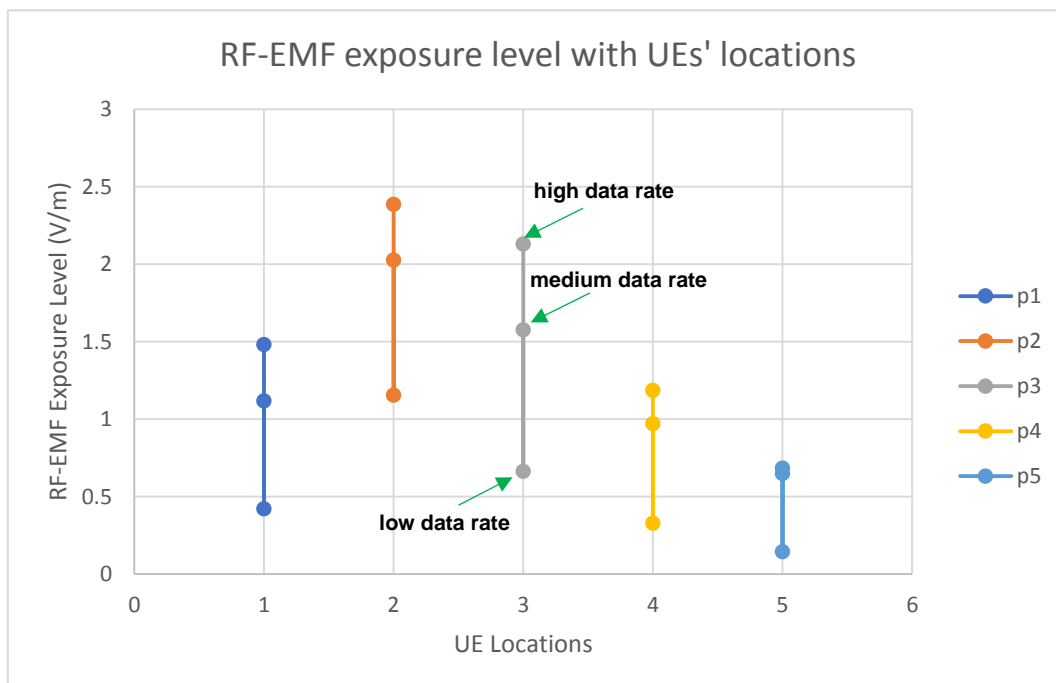


Figure 41 Empirical RF-EMF exposure levels acquired at each UE location for the targeted 'high',

'medium' and 'low' data rate levels (i.e. 700 MHz, 350 MHz and 70 MHz, respectively).

As depicted in Figure 31, the distance of UE away from the Keysight RF-EMF measurement probe are in the order of UE2, UE3, UE1, UE4 and UE5. When UE2 is activated, the probe can obtain the highest RF-EMF exposure level at the three targeted data rate levels. This coincides with the proximity of the Keysight RF-EMF measurement probe position at UE2. For UE1 and UE3, whose beam directions are closer to the probe's direction than UE4 and UE5. The beam direction spacing of UE5 is the largest, so the RF-EMF exposure level measured by the probe is the smallest.

6 Conclusion

This report has presented work focus on using a fully controlled mMIMO system to evaluate the measurement protocols and processing methods for rigorous RF-EMF assessments in the context of 5G mMIMO base station applications. Both indoor and outdoor measurement campaigns have been carried out. Given the statistical nature of the mMIMO transmission, where the spatial pattern of transmission (i.e. number of beam used, direction of the beams) can change every few milliseconds, it makes some sense that the new metrology for 5G BS is based on statistical RF-exposure models, either based on system level simulations or real measurement data acquired from deployed 5G BS. Some evidences already point out that such model provides realistic and implementable exclusion zones for 5G BSs. However, more works need to be done to fully understand the spatial and temporal variations of the RF-exposure and make these existing statistical models more accurate and robust in any environment/scenario.

This leads to the usage of an mMIMO testbed with fully reconfigurable capability for acquiring more relevant measurement in various environments/scenarios and, then, refining/strengthening the statistical RFexposure model for 5G BS, based on the following findings:

- (1) the RF exposure decays in a quadratic manner as a function of the distance, even when there is no main beam pointing directly into this direction;
- (2) the peak of the RF exposure at a particular point in space is reached as an active beam is directly steered towards it;
- (3) more than one peak of the RF-exposure may be observed for single user test case if there is multipath effect (e.g. due to reflecting object in close proximity to the UE terminal);
- (4) the overall RF-exposure at a given point increases with the number of users that are served simultaneously by the mMIMO BS and this effect is more significant close to the mMIMO BS than further away;
- (5) the RF-exposure of a mMIMO BS varies significantly as a function of the amount of data it transmits and the number of active antenna element from the mMIMO BS;
- (6) the SSB based method could be used to evaluate the RF-EMF level as the field strength method without going through vast data rate samples.

The relevant statistical analysis based on these experimental-based evidences have been performed to enable the insight understanding. The outcomes of this work are envisaged to enable refinement of the developed RF-EMF measurement and data processing method for 5G NR Massive MIMO base stations. In turn, this will form the basis of the recommendations to the technical, business and regulatory communities.

7 References

- [1] A. Osseiran, J. F. Monserrat, P. Marsch, *5G Mobile and Wireless Communications Technology*, Cambridge University Press, Jun. 2016.
- [2] ICNIRP, “Guidelines for limiting exposure to electromagnetic fields (100 kHz to 300 GHz)”, *Health Phys.*, Vol. 118, No. 5, pp. 483–524, Mar. 2020.
- [3] B. Thors, A. Furuskär, D. Colombi, and C. Törnevik, “Time-Averaged Realistic Maximum Power Levels for the Assessment of Radio Frequency Exposure for 5G Radio Base Stations Using Massive MIMO”, *IEEE Access*, Vol. 5, pp. 19711 – 19719, Sept. 2017.
- [4] P. Baracca, A. Weber, T. Wild and C. Grangeat, “A Statistical Approach for RF Exposure Compliance Boundary Assessment in Massive MIMO Systems”, *the 22nd International ITG Workshop on Smart Antennas (WSA 2018)*, 2018, pp. 1-6.
- [5] C. Törnevik, “Impact of EMF limits on 5G network roll-out”, *ITU Workshop on 5G, EMF & Health 2017*, Warsaw, Poland, Dec. 2017.
- [6] 5G Innovation Centre, University of Surrey, “System Level Massive MIMO Testbed”, *Forum Europe EMS 2016*, Apr. 2016 [Online]. Available: https://eu-ems.com/event_images/presentations/Dr%20Mir%20Ghoraishi%20presentation%20-%20Massive%20MIMO%20demo.pdf.
- [7] N9917B FieldFox Handhold Microwave Analyser, Keysight [Online]. Available: <https://www.keysight.com/en/pdx-2979921-pn-N9917B/fieldfox-handheld-microwave-analyzer-18-ghz?nid=-32505.1268855&cc=US&lc=eng>.
- [8] SDIA-6000 Triaxial Isotropic Antenna, Sysdyne Advanced Technologies Co., Ltd. [Online]. Available: http://sysdyne.co.kr/en/?page_id=1091.
- [9] NPL Power Flux Density Laboratory [Online]. Available: <https://www.npl.co.uk/products-services/radiofrequency/pfd-andfield-strength>.
- [10] T. H. Loh, F. Heliot, D. Cheadle, T. Fielder, "An Assessment of the Radio Frequency Electromagnetic Field Exposure from A Massive MIMO 5G Testbed", *the 14th European Conference on Antennas and Propagation (EuCAP 2020)*, Copenhagen, Denmark, 15 – 20 Mar. 2020.
- [11] T. H. Loh, D. Cheadle, F. Heliot, A. Sunday, and M. Dieudonne, "A Study of Experiment-based Radio Frequency Electromagnetic Field Exposure Evidence on Stochastic Nature of A Massive MIMO System", *the 15th European Conference on Antennas and Propagation (EuCAP 2021)*, Düsseldorf, Germany, 22 – 26 Mar. 2021.
- [12] Keysight PathWave System Design (SystemVue) [Online]. Available: <https://www.keysight.com/gb/en/products/software/pathwave-design-software/pathwave-system-design-software.html>.
- [13] 5G Verticals Innovation Infrastructure (5G-VINNI) [Online]. Available: www.5g-vinni.eu.